

Optical discharges

Yu. P. Raizer

Institute of Mechanics Problems of the USSR Academy of Sciences
Usp. Fiz. Nauk **132**, 549–581 (November 1980)

Gas breakdown, steady-state maintenance and the continuous generation of a low-temperature plasma, and propagation of the plasma fronts, all are induced by laser radiation. By nature, and in conformity with the fundamental laws, these effects are not different from similar processes that occur in constant and alternating fields and which are a traditional subject of the study of the physics of gas discharge. In fact, a new chapter has been added to the gas-discharge sciences: discharge at optical frequencies. It is a rapidly developing new field which encourages both new experiments and applications. It appears useful at this time to characterize the position occupied by the new field within the general framework of discharge sciences, and to analyze and appraise the latest results.

PACS numbers: 51.70. + f

1. POSITION OF THE OPTICAL DISCHARGES AMONG OTHER DISCHARGE PHENOMENA

(a) Frequency ranges

During the "pre-laser" era and, more precisely, up to the mid-60's, the physics and technology of gas discharge were committed to fields in three basic frequency ranges: (1) constant electric fields with which, depending on the nature of interaction, relatively short-lived pulsed fields and low-frequency oscillating fields are partially conformable, (2) high frequencies (called "radio frequencies" in the foreign literature), a broad range with a mean around 1 MHz, and (3) superhigh frequencies, designated SHF (called "microwaves" in the foreign literature) and to be found in the gigahertz region that corresponds to the centimeter and millimeter waves. Beyond these lies the optical region: infrared, visible and ultraviolet radiation. However, during the pre-laser era—characterized by weak conventional, non-laser, light sources and the fields they produced—the possibility of occurrence of gas-discharge effects in the light fields was beyond everyone's comprehension.

Historically, gas-discharge phenomena were explored in general in the order of ascending frequency ranges. Thus, constant or short-lived fields generated by condenser discharges were investigated first (hence, incidentally, the term "discharge" which applies to processes occurring in the gas portion of a circuit). Toward the end of the last century and the early part of this century, attention had shifted to rf fields. The early 1940's and the development of rocket technology had advanced the range to microwaves. And, finally, the mid-1960's have moved the field into the optical range.

The development of relatively powerful pulsed and cw lasers had enhanced the discovery and investigation of the many new phenomena induced in a gas by laser radiation, and the interaction of the latter with ionized gases and plasmas. Upon closer examination, it becomes evident that among these effects there are specific processes which naturally and fully belong to gas-discharge physics. The laser technology has essential-

ly bequeathed to the discharge physics a fourth, optical range, thus intrinsically endowing this science with a fundamentally new, exceptionally interesting and highly applicable chapter that deals with discharges in optical fields. Conceivably, the new term—optical discharge—sounds alien to many at this time, but, in fact, it conveys as much sense as the time-honored terms "radio frequency" or "microwave" discharges. The new chapter occupies a proper place among the gas-discharge sciences, and it entails the same fundamentals as the chapters on radio-frequency and microwave discharges.

(b) Classification of "discharge processes"

For simplicity, and in order to clarify the position that effects, arising from the interaction of laser radiation with the ionized gases, occupy among the conventional gas-discharge phenomena, it is expedient to classify all gas-discharge phenomena in some meaningful way. Bearing in mind that the interaction of laser radiation with a gas is unaffected, as a rule, by the presence of solid surfaces, the effects must be classified according to criteria which are dissociated from the effects of electrode-, near-electrode- and boundary-intensive processes. We shall distinguish three basic types of spatial gas-discharge processes:

(1) Gas breakdown, development of a turbulent avalanche ionization in it due to an applied external field, and conversion of initially non-ionized gas into a plasma.

(2) Maintenance of an unstable plasma by a field, in which the temperature of electrons responsible for the ionization is sufficiently high, and the gas containing atoms, molecules and ions remains cold. Normally, this corresponds to a weakly-ionized plasma at fairly high pressures, below 100 torr. The degree of ionization is, moreover, much lower than a value for a stable plasma, which corresponds to electron temperature.

(3) Maintenance of a stable plasma by a field, in which the electron and heavy-particle temperatures are close, and the degree of ionization is close to that of a thermodynamically stable plasma. This is a so-

TABLE I.

Field frequency range \ Type of discharge plasma	Breakdown	Maintenance of an unstable plasma	Maintenance of a stable plasma
Constant electric field	In interelectrode gaps	Glow discharge	D.C. arc
Radio frequencies	Radio frequency, electrode or electrodeless	Radio frequency moderate-pressure capacitive discharge	Inductive discharge at atmospheric pressure
Microwave frequencies	In waveguides and resonators	Pulsed discharges in waveguides and resonators	Microwave plasmotrons
Optical frequencies	In gases, induced by a focused laser pulse	Late stages of an optical breakdown	Cw optical discharge, maintained by a CO ₂ gas laser radiation

called low-temperature plasma with temperatures of the order of 10,000 K, and at pressures normally of the order of atmospheric.

Each of these processes may occur in any of the foregoing frequency ranges. In fact, nearly all the possible alternatives have been investigated experimentally, and many of these have been found to have occasionally important research and engineering applications. Table I above illustrates the adopted classification, and indicates typical conditions under which one or another process is observed.

(c) Purpose of the paper

Below, we shall consider processes that are induced by laser radiation and belong to the category shown in the bottom line in the table. Having analyzed the salient points, we shall show the gas-discharge nature of these processes and verify that, in principle, they hardly differ from other processes in the same category. We shall also review the current status of investigations and results in this area. The first problem calls for a brief digression into the realm of well-known concepts. The second pertains basically to results obtained after 1972-1973, which were excluded from the author's monograph published in 1974 (Ref. 1).

2. OPTICAL GAS BREAKDOWN

(a) Discovery

The instant of birth of the new chapter of gas discharge physics is etched in the memory of many physicists of the present generation. It is associated with the discovery of a remarkable effect: optical gas breakdown. The first to report this effect were Maker, Terhune and Savage in February 1963.²

The discovery of the effect was made possible by the invention of the Q-switched laser, which is capable of producing an especially powerful, so-called giant pulse. When the beam of such a (ruby) laser was focused by a lens, a spark occurred in the focal region, producing a plasma there, as in the case of breakdown in the discharge gap between electrodes (Fig. 1). Very high radiation parameters are required to break down the free air by optical radiation. Air breaks down at the peak power of 30 MW and when a beam is focused to a spot

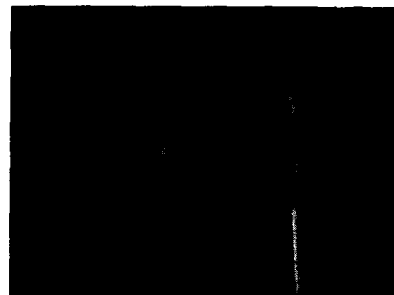


FIG. 1. Photograph of a laser spark.

10⁻² cm in diameter (the typical duration of a giant pulse is 30 ns = 3 × 10⁻⁸ s; the energy in such a pulse is 1J). The flux density at the focus for these parameters is 10⁵ MW/cm², and the electric field intensity in the electromagnetic wave is approximately 6 × 10⁶ V/cm.¹⁾ The breakdown threshold is well defined, and a small decrease in the flux density below a given value will preclude breakdown.

The new effect had evoked such broad interest among physicists that they literally rushed to investigate it. During the next several years, optical breakdown was being studied experimentally and theoretically with such intensity of detail that today our knowledge about it is as extensive as is our understanding of its closest analog, the microwave breakdown, and is certainly superior to our understanding of a more complex process, breakdown of a relatively long gap between electrodes. The bulk of materials dealing with the optical breakdown was generated during the 1960's, as was also the theory of the phenomenon.¹ In recent years, little was added to these data in the way of fundamental knowledge, although some additional experimental numbers have been calculated, refinements of the theory carried out, and allowances for certain subtle and understood details made.

Figure 2³ shows the threshold fields in an optical wave E_t , which are required to break down several gases by focused radiation from a ruby laser. The threshold values were measured over a broad range of pressures p . By way of comparison, Fig. 3 shows similar data pertaining to breakdown due to microwaves.⁴ The overall similarity of the $E_t(p)$ curves should be underscored. As we shall see further, this property has a profound physical meaning.

(b) Avalanche ionization in a field

An electron avalanche develops in a gas under the effect of an electric field associated with an optical wave, as it also does during breakdown in any other field. In the case of breakdown induced by ultrashort pulses from ruby and neodymium-glass lasers, the first, priming electrons appear as a result of a multiphoton emission from atoms, molecules and, possibly, dust which is present in the gas. In this respect,

¹⁾ In a constant field, free air breaks down at the field intensity of 3 × 10⁴ V/cm.

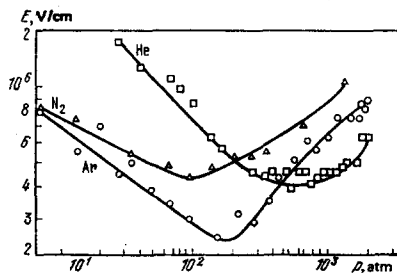


FIG. 2. Thresholds for a ruby-laser-induced breakdown in Ar, He, and N₂. Pulse duration 50 ns, focal spot diameter 10⁻² cm (Ref. 3).

breakdown in the optical field differs from breakdown in fields of lower frequency, in which the first electrons appear at random (from cosmic rays). Inside the wave field, an electron gradually acquires energy due to collisions with atoms, and it becomes sufficiently energetic to ionize an atom and to produce a new electron. This is the mechanism of electron multiplication.

Avalanche development is determined by an interplay of two opposing processes: energy accumulation by electrons due to the field and energy loss by electrons due to collisions (elastic and inelastic). It is also determined by a loss of electrons due to diffusion or sticking in electronegative gases. Loss of both energy and electrons is relatively independent of the nature of a field, and it occurs in a manner that is more or less the same for all fields. Energy acquisition is the only frequency-dependent process whereby singular features of the optical breakdown, which are associated with the quantum nature of interaction between light and electrons, may be revealed.

In an alternating field, electrons pursue both oscillatory and random motion. According to classical theory, each collision of an electron with a molecule or atom results in a transfer of the mean energy of an oscillating electron $\Delta\varepsilon = e^2 E^2 / m \omega^2$ into the energy of random motion ε (E is the mean-square electric field and ω is angular frequency). This occurs provided the collisions are relatively infrequent. However, if an electron fails to undergo many oscillations during a period between collisions, i.e., each time oscillations fail to swing "fully," energy transfer from the field to electrons is slowed down. In the general case, the field imparts the following energy per second to an electron

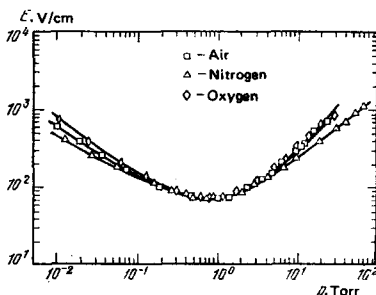


FIG. 3. Breakdown thresholds for N₂, O₂, and air in a microwave field. Frequency 0.994 GHz, diffusion length of discharge volume 1.51 cm (Ref. 4).

$$\left(\frac{d\varepsilon}{dt}\right)_E = \frac{e^2 E^2}{m(\omega^2 + \nu_m^2)} \nu_m, \quad (1)$$

where ν_m is the effective frequency of electron collisions with molecules.

Inasmuch as the collision rate is proportional to gas density or pressure, the rate of energy build-up due to the field for each frequency ω at relatively low pressures is proportional to pressure p , and is determined by the ratio E/ω . At relatively high pressures, it is inversely proportional to pressure and independent of ω :

$$\begin{aligned} \text{at } \nu_m^2 \ll \omega^2 \quad \left(\frac{d\varepsilon}{dt}\right)_E &\sim \left(\frac{E}{\omega}\right)^2 p, \\ \text{at } \nu_m^2 \gg \omega^2 \quad \left(\frac{d\varepsilon}{dt}\right)_E &\sim \frac{E^2}{p}. \end{aligned} \quad (2)$$

(c) Threshold field

In order that an avalanche may develop and breakdown take place, energy losses by electrons and a loss of electrons must be surmounted. In the case of very short field pulses, another requirement is that an appreciable level of ionization must be attained within the pulse width, such that a sufficient number of electron generations is produced. Clearly, an appropriately high rate of energy conversion is required to accomplish this, which is sufficient to provide the required gas ionization frequency ν_i . The latter is the reciprocal of time an electron needs in which to attain energy greater than the ionization potential and to produce ionization. Thus, the breakdown criterion places a specific condition on the parameters $(d\varepsilon/dt)_E$ and $E = E_t$.

Consequently, at low pressures, when $\nu_m^2 \ll \omega^2$, the breakdown threshold field E_t is proportional to frequency and decreases with increasing pressure. Conversely, at high pressures, when $\nu_m^2 \gg \omega^2$, the threshold field, grows with increasing pressure and only weakly depends on the frequency. In alternating fields, the breakdown threshold is minimal at pressures that approximately satisfy the condition $\nu_m = \text{const } p \approx \omega$. These considerations explain the behavior of curve $E_t(p)$ in Fig. 3 for a microwave breakdown.²⁾

The behavior of the optical breakdown curve may be explained in the same qualitative way (see Fig. 2). If we proceed from the same equation [Eq. (1)], it becomes evident why breakdown at optical frequencies requires fields considerably stronger than at microwave frequencies ($E_t \sim \omega$, threshold intensity of electromagnetic wave $S_t \sim E_t^2 \sim \omega^2$). It becomes clear why the $E_t(p)$ minimum shifts in the direction of high pressures the order of hundreds of atmospheres (the minimum occurs at $p \sim \omega$). The main issue is to what extent the applicability of Eq. (1) is validated for the quantum case of optical frequencies.

(d) Classics and quanta

The possibility of using a simple and clear formula [Eq. (1)] in the case of optical frequencies was validated

²⁾ Incidentally, the shape of the right-hand side (ascending) branch is, in general, similar to the right-hand side (ascending) branch of the Paschen curve for the breakdown of a gap between electrodes to which a voltage was applied.

in one of the first works dealing with the optical breakdown⁵ in which a quantum theory of this effect was formulated. Actually, an electron absorbs energy in quanta, i.e., significant amounts of $\hbar\omega$ equal to 1.78 eV for a ruby laser and 1.17 eV for a neodymium-glass laser. Moreover, the actual energy $\hbar\omega$ acquired by an electron during collision with an atom is much greater than $\Delta\varepsilon = e^2E^2/m\omega^2$, the collisional energy that an electron would have received according to the classical theory. It would seem the latter is totally inapplicable under these conditions.

However, analysis of the quantum kinetic equation for the electron energy distribution function shows that Eq. (1) may be used anyway, even if the actual classical condition $\hbar\omega \ll \Delta\varepsilon$ is not satisfied. This requires a much less stringent condition $\hbar\omega \ll \varepsilon$, where ε is the actual electron energy. In the microwave range, even the trivial requirement $\hbar\omega \ll \Delta\varepsilon$ is satisfied and the question of quantum effects does not generally arise. Conversely, in the optical range, $\Delta\varepsilon \sim 10^2$ eV $\ll \hbar\omega \sim 1$ eV; however, the mean energy of electron spectrum is of the order of the ionization potential, i.e., 10 eV and, therefore, the condition $\hbar\omega \ll \varepsilon$ may be considered satisfied, at least for the frequencies of ruby and neodymium-glass lasers.

Thus, in the case of optical fields, Eq. (1) roughly holds, although it should be treated statistically. Let, for example, $\Delta\varepsilon = 0.01 \hbar\omega$. An electron, of course, may not receive a hundredth of a photon from the field during collision. This means that, roughly speaking, it gains nothing in the first 99 collisions, and in the hundredth collision it absorbs a full photon all at once. Strict calculations of the electron avalanche and breakdown threshold are normally carried out on the basis of the kinetic equation. Calculations carried out in Ref. 5 and subsequent works (see Ref. 1) are in satisfactory agreement with experimental results.

Alongside the many classical characteristics, certain new details also appear at optical frequencies, which are associated with the quantum nature of interaction between the optical radiation and matter. Thus, for example, ionization of excited atoms is possible by means of two- or three-photon emission of electrons and this sometimes significantly affects the multiplication rate for electrons. However, the avalanche mechanism of the optical breakdown is neither different in principle from a mechanism responsible for microwave breakdown, nor from a spatial breakdown at lower frequencies, including the Townsend (not streamer) gas discharge between electrodes.

(e) A link between microwaves and light

A particularly convincing experimental result in this respect is the fact that the classical laws $E_t \sim \omega$ or $S_t \sim \omega^2$ are satisfied for the threshold values over a broad range of optical frequencies, up to the microwave range. As far as the latter is concerned, the law $E_t \sim \omega$ is theoretically valid only at low pressures that correspond to the left-hand side of the curve $E_t(p)$. However, even the atmospheric pressure in the optical region is "low" in this sense.

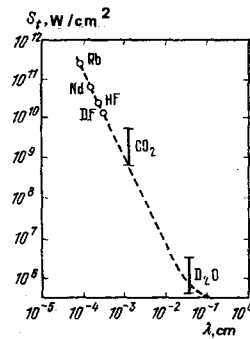


FIG. 4. Thresholds for atmospheric-pressure air breakdown induced by various lasers. Dashed line corresponds to the classical function $S_t \sim (\omega^2 + \nu_m^2)$ which, with the exception of very long-wave region, yields a law $S_t \sim \omega^2$, i.e., a straight line in the logarithmic scale.

To validate the law, we have numerous data for the air breakdown by ruby ($\lambda = 0.694 \mu\text{m}$), neodymium-glass ($\lambda = 1.06 \mu\text{m}$) and CO_2 ($\lambda = 10.6 \mu\text{m}$) lasers. Quite recently, other results were obtained in the intermediate infrared range by means of HF ($\lambda = 2.7 \mu\text{m}$) and DF ($\lambda = 3.8 \mu\text{m}$) lasers,⁶ and a heavy water laser ($\lambda = 385 \mu\text{m} = 0.38 \text{ mm}$) was used to establish a point in the broadest unknown region of the spectrum between the infrared and microwave regions (the submillimeter region).⁷

Threshold intensities are shown on a logarithmic scale in Figure 4; the experimental data points are plotted on the curve which follows the law $S_t \sim \omega^2$. As can be seen, data points bunch closely near the curve, although strict obedience of the law is never expected. The fact is that work with different lasers is performed under different experimental conditions. The pulse width of ruby and neodymium-glass lasers is approximately 30 ns; CO_2 laser, in this case, 80ns; HF, 120ns; DF, 90ns; and D_2O , 75ns. The focal spot diameters are also different (10^{-2} – 10^{-3} cm). At the long wavelength, threshold essentially depends on either presence of dust particles in the air or the preionization conditions, since the occurrence of priming electrons in these cases is difficult. Deviation of a point at $\lambda = 0.38 \text{ mm}$ from the curve $S_t \sim \omega^2$ is associated with the fact that the frequency ω is already comparable with collisional frequency ν_m and the law must be corrected for the latter [$S_t \sim (\omega^2 + \nu_m^2)$]. Allowance for this makes the theory more compatible with experiment.

The law $S_t \sim \omega^2$ is violated significantly in the short-wave region of the spectrum as a result of breakdown by the second harmonics of neodymium-glass and ruby lasers. Instead of increasing, the threshold intensity decreases sharply with increasing frequency (quantum growth). Here, quantum effects are fully in evidence; the second harmonic of a ruby laser is very large, 3.56 eV.

(f) A long spark

At a moderately high intensity above threshold, laser radiation must be sharply focused to produce breakdown, which occurs only in a small focal region. However, at very high intensities in the case of a beam

weakly collected by a long-focus lens, the intensity is sufficient to produce air breakdown over a long distance along the lens axis and beyond. This results in an extended optical breakdown, a highly impressive phenomenon called the "long spark."

A two-meter long spark was observed for the first time in 1967, when a 1-GW 18-ns giant-pulse neodymium-glass laser was focused through an $f=2.5$ -m lens.⁸ Two years later, a 25-m spark was produced [by a 90-J 4-GW(peak) neodymium-glass laser, with a beam divergence of 4×10^{-5} rad and focused by a $f=28$ -m lens].⁹ A 15-m section of the spark extended in front of the focus and a 10-m section, behind. A record-length spark—longer than 60 m—was obtained in 1976 by means of a two-stage neodymium-glass laser setup, with the combined energy of 160J and average power of 5GW, using an $f=40$ m lens.¹⁰ The spark, produced in a courtyard (at an institute) is well defined against the background of a building (Fig. 5). Long sparks are never continuous, but consist of ionized sections alternating with those unaffected by breakdown. Clearly, this is associated with the statistical origin of the priming electrons which occur at selected points and, probably, the time-dependent variations in the field at various points due to a complex spatial-temporal and angular structure of the intense light beam.

Long sparks were also obtained in air by means of high-power electroionization CO₂ lasers^{11,12} (of the order of 1 m¹¹). The purpose of one work¹² was to establish the maximum power and intensity of the CO₂ laser radiation that can be propagated through air, a problem of considerable importance. The laser output was 160J, of which 30J was produced during 50 ns and the remainder, 130J, during μ s; the peak power was 0.56 GW. The longest spark (7.5m) was achieved by expanding the initial beam by means of a telescope to be 40 cm in diameter and, subsequently, focusing it by means of a long-focus mirror ($f=54$ m) directly outdoors; the angle of beam convergence (d/f) was 1/135 and the least cross-section diameter, 0.5 cm. The spark occurred at intensities of $1 - 2 \times 10^9$ W/cm². A considerable portion of radiation (of the order of tens of percent) was absorbed in the process by the plasma. Both the plasma generation threshold and amount of

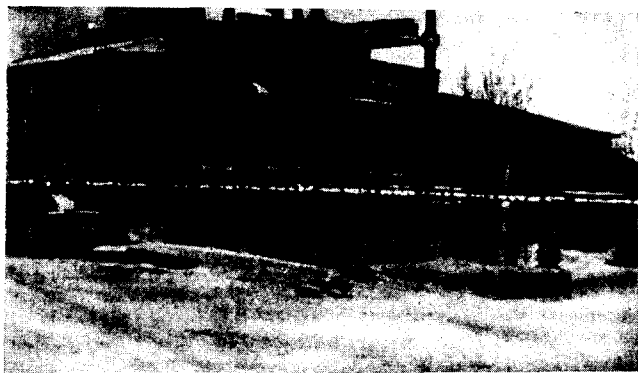


FIG. 5. Photograph of a long spark obtained by means of a neodymium-glass laser. Spark length 8 m, focal length of lens 10 m (Ref. 10).

energy absorbed in the plasma depend on the dust content of air, the presence in air of sub-micron size aerosol particles, and humidity. In purified air, the threshold increases to 3×10^9 W/cm². Schlieren photography shows that each particle serves as a plasma focus from which an optical detonation wave propagates (see below) and leaves an absorbing plasma cloud behind it.

Actually, the plasma generation threshold measured in the experiment (10^8 W/cm²) is not the same as the breakdown threshold, i.e., occurrence of avalanche ionization in a gas induced by a priming electron; the latter is an order of magnitude higher. Instead, it represents a threshold at which the plasma foci occur as a result of heating of gas particles and the subsequent ionization of ambient air by laser radiation. The question of what is the real mechanism for breaking down dusty air by CO₂ laser radiation remains unclear. Citations concerning this subject may be found in Refs. 12 and 13. The breakdown threshold is further reduced if the radiation is focused near a solid surface.^{14,15} (and references therein)

(g) Discharge initiation by a laser spark

It was observed some time ago that concurrent interaction of the laser radiation and other fields—microwave, constant—with a gas considerably enhances its breakdown by the other field. In this manner, directed breakdown is achieved between electrodes under a constant potential: The spark discharge develops along the optical channel and may be directed either at an angle to the constant field or even be fractured (for references see Refs. 1 and 11). The lowering of the electric breakdown threshold and a very rapid laser interaction effect have contributed to the development of laser-fixed dischargers.¹⁶ The long laser spark has been used effectively to initiate discharge in long interelectrode gaps.^{11,17-19} This procedure may replace the conventional method of using thin exploding wires for initiating electrical discharges, which has many disadvantages. The long laser-spark path provides a conduit for the electrode gap discharge. Moreover, breakdown electric field intensity is reduced considerably to 250V/cm.¹⁹ Normally, electric breakdown of long gaps is due to a leader mechanism: A bright channel leader, propagates from the anode, and is preceded by a darker streamer. The dense portion of a long laser spark, which lies relatively close to the focus, is an equivalent of a leader thus formed.¹⁹

3. MAINTENANCE OF AN UNSTABLE PLASMA

Glow discharge is one of the most common discharge processes in a constant field at pressures below tens of torr. Unstable, weakly-ionized stationary plasmas may be produced at both radio and microwave frequencies at low pressures. At optical frequencies, however, the steady-state process is totally atypical; instead, it calls for much higher radiation intensities. The power of currently available cw lasers is sufficient, as a rule, to maintain a stable plasma only.

Steady-state maintenance of an unstable plasma al-

ways requires electric fields that are considerably stronger than those used to maintain a stable plasma. This applies in general to all frequency ranges including the optical. Actually, energy which an electron receives from the field is transported without delay to atoms, molecules and ions. The electron temperature T_e rapidly assumes a steady-state value which is determined by a balance between an average energy acquisition from the field, and transfer to heavy particles during each collision:

$$\frac{e^2 E^2}{m(\omega^2 + \nu_m^2)} = \delta \cdot \frac{3}{2} k(T_e - T); \quad (3)$$

where T is temperature of heavy-particle gas, and δ is average portion of energy given up by an electron to heavy particles when $T_e \gg T$. In an atomic gas, $\delta = 2m/M \sim 10^{-5} - 10^{-4}$ (M is atomic mass); in a molecular gas, because of inelastic processes of excitation of vibrations and rotations, $\delta \sim 10^{-3} - 10^{-2}$.

In order that the electron-shock ionization of atoms—the rate of which rapidly increases with T_e —could make up for electron losses and the plasma remain intact, the electron temperature in any discharge, both stable and unstable, must be maintained at approximately 1-eV level. In a stable plasma, for which $T_e - T \ll T_e$ and the energy exchange between electrons and molecules is bilateral, the required field is much smaller than in an unstable plasma, where $T_e \gg T$ and the electrons only yield energy to molecules and receive nothing from them. In the unstable case, Eq. (3) defines the field required to maintain a plasma. In the stable case, field is defined by the overall energy balance of the entire plasma (see Section 4), and Eq. (3) fixes only a small detachment of temperature ($T_e - T$) being established. Equation (3) may be used to estimate the required CO_2 -laser radiation intensity readily for the steady-state maintenance of an unstable plasma with $T_e \gg T$. We have $\omega = 1.78 \times 10^{14}$ rad/s, and for $p < 10$ atm, $\omega^2 \gg \nu_m^2$, i.e., E and $S = cE^2/4\pi$ are independent of pressure. Let $T_e = 1.5$ eV; $\delta = 2.7 \times 10^{-5}$ and $S \approx 3 \times 10^8$ W/cm² in argon and $\sim 0.8 \times 10^{12}$ and $\sim 10^9$ W/cm² in air, respectively. These values are very high for cw lasers, the latter even exceeding the breakdown threshold for natural free air. However, in order that a discharge be prevented from spontaneously becoming stable, rapid extraction of energy from the gas is necessary, for which lower pressures are preferred (as also in the case of all unstable discharges).^{20, 3}

Thus, although there exists in principle a possibility of a steady-state maintenance of an unstable plasma by light, application of this process is difficult. The process is also "unprofitable:" A weakly-ionized plasma absorbs only a small portion of radiation, unless it is produced along a very long and powerful optical beam.

³⁾ The fact that $E_{\text{unstable}}^2 \gg E_{\text{stable}}^2$ does not mean that more energy is released in an unstable plasma than in a stable plasma. The energy yield density is proportional not only to E^2 , but also the electron density n_e . The unstable plasma is always weakly ionized: In the case of strong ionization the energy yield is somewhat large, the heat transfer is unable to prevent heating of the gas to the electron temperature level, and the plasma becomes stable.

Although experiments of this kind have not been tried, the effect occurs automatically for short periods of time in the terminal stage of the optical breakdown at near-threshold powers.

4. STEADY-STATE MAINTENANCE OF A STABLE PLASMA

(a) Continuous optical discharge and the optical plasmotron

Discharges of the arc type, in which a stable plasma is maintained in a steady state by a field, have broad application in physical research and engineering. Generators which produce dense low-temperature plasmas—plasmotrons—are built on this basis. In a plasmotron, cold gas is blown through a steadily burning discharge. The gas is heated to temperatures of 5000–10,000 K, and flows out as a continuous plasma jet, more often at atmospheric pressure. Today, fields are used in laboratories and industrial equipment which fall into three frequency ranges: constant, rf and microwave. Accordingly, there are three types of plasmotrons: arc, induction and microwave.

In 1970, the possibility of steady-state maintenance of a plasma by cw laser radiation was articulated and theoretically validated, and thoughts concerning the design of an optical plasmotron based on this principle were expressed.²¹ A continuous optical discharge—as it was called—was obtained experimentally the same year by means of a cw CO_2 laser.²² In terms of determining processes, the continuous optical discharge was similar to static stable discharges occurring in any other fields. Energy release in a plasma due to absorption of the optical wave makes up for the losses associated with energy discharge due to thermal conduction and radiation. Not unlike electrical conductivity, light absorption coefficient depends on both temperature and pressure under equilibrium conditions. The temperature of a steady-state plasma is determined by the need for the precise compensation of energy lost and energy released, and for stability of the state.

But, of course, plasma maintenance by laser is characterized by special features which are associated with the radiation properties of the optical region, the principal among these being a capacity to transfer optical energy freely over distances. If the delivery of energy to a plasma in all other fields requires the use of specific structural components—such as electrodes in an arc discharge, an induction coil for rf, and a waveguide for microwaves—a light beam may deliver energy directly through air. This opens vast possibilities for initiating an optical discharge in virtually inaccessible places or directly in the middle of a room. The plasma may be set in motion in space by translating the light beam and thereby tracing "plasma patterns" in the space. Gas may be blown across a discharge, thus obtaining an optical plasmotron. In case of the latter, as also in all existing plasmotrons, the electromagnetic energy supplied from outside is ultimately spent on heating successively new batches of incoming cold gas to a high temperature.

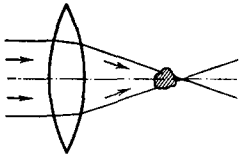


FIG. 6. Diagram of an experimental setup for obtaining a continuous optical discharge. Plasma is displaced from focus toward beam.

In practice, optical discharge is induced at a specific location by focusing a laser beam with a lens or mirror. The plasma lies near the focus where the intensity of light is high. It is slightly shifted from the focus toward a source of radiation, up to a cross-section of the light cone where intensity is still sufficient to support burning of a discharge (Fig. 6). In order to ignite a steady-state discharge, it is necessary to produce initial plasma in the focal region, because the beam power required to maintain an existing plasma is far too small to generate it, i.e., to produce a gas breakdown (as the case is with all other steady-state discharges). It is possible, for example, to produce gas breakdown at a focus by means of an outside source; the simplest way to do it is to insert a wire into the focal region for a short time, and to remove the same after a discharge has ignited.

(b) Determination of the plasma temperature and threshold power of light

The fundamental problem in the theory of stable discharges is the determination of the plasma temperature as a function of the strength of applied field (and other conditions). This requires solving a coupled system of energy balance equations for the plasma and field. Normally, efforts are made to simplify the equations by first simplifying the discharge geometry. Thus, for example, an arc between electrodes or an inductive discharge inside a solenoid can be modeled by an infinitely long plasma cylinder. This procedure reduces the problem to the one-dimension case.

The geometry of an optical discharge is highly complex and, at least, two-dimensional (see Fig. 6). However, having interest in the lowest beam powers that will support a discharge, i.e., conditions at which the plasma is centered near the focus, for the purpose of calculation, the plasma formation may be considered to be a sphere in which a spherically-symmetric converging laser beam with power P_0 is partially absorbed. Moreover, in the case of extremely small dimensions (large temperature gradients) and relatively low pressures ($p < 5$ atm), radiative losses are small in comparison with energy lost by the plasma due to thermal conductivity, and may be neglected.

In a highly ionized gas the infrared radiation of a CO_2 laser is absorbed in the course of collisions between electrons and positive ions (in a process which is the opposite of bremsstrahlung). The absorption coefficient μ_ω is proportional to densities of colliding particles, $\mu_\omega \sim T^{-3/2} n_e n_+^{-1}$. In the case of partial single ionization $n_e n_+ \sim \exp(-I/kT)$; moreover, the ionization potential

$I \gg kT$, such that μ_ω increases very sharply with increasing temperature. When practically all atoms are singly ionized, the coefficient of absorption at a constant pressure goes through a maximum and, subsequently, decreases with increasing temperature until such time as second ionization takes place. Actually, in the case of total single ionization and $p = (n_e + n_+)kT = 2n_e kT = \text{const}$, we obtain $\mu_\omega \sim T^{-7/2} p^2$.

Let the temperature at the center of the plasma be T_K ; the temperature falls off from the center along the radius r . We shall introduce a certain ionization temperature T_0 , below which the ionization is sufficiently low to neglect absorption. We shall denote the sphere radius by r_0 , where $T = T_0$, and call Θ potential of the thermal flux J . If λ is thermal conductivity coefficient

$$J = -\lambda \frac{dT}{dr} = \frac{d\Theta}{dr}, \quad \Theta(T) = \int_0^T \lambda(T) dT.$$

Let the portion of laser power absorbed in the sphere be P_1 . On the outside, for $r \geq r_0$, where no energy is released, $4\pi r^2 J = \text{const} = P_1$, such that

$$\Theta(r) = \frac{P_1}{4\pi r}, \quad P_1 = 4\pi r_0 \Theta_0, \quad \Theta_0 = \Theta(T_0). \quad (4)$$

The thermal flux carried power P_1 out of the sphere. At comparatively low, near-threshold powers P_0 , the plasma dimensions are small and it remains transparent to laser radiation. Under these conditions, energy is released throughout the sphere and the order of magnitude of $P_1 \approx 4\pi r_0^2 \Delta\Theta / r_0 = 4\pi r_0 \Delta\Theta$, where $\Delta\Theta = \Theta_K - \Theta_0$ is the potential difference between the center of the sphere and the outside. Comparing this equation with Eq. (4), we find that $\Delta\Theta \approx \Theta_0 \approx \Theta_K / 2$ and $P_1 \approx 2\pi r_0 \Theta_K$. But, in the case of a transparent plasma $P_1 \approx \mu_\omega r_0 P_0$, where the absorption coefficient μ_ω , averaged over the radius r_0 , will refer approximately to temperatures at the center T_K . The last two equations yield a relationship between the plasma temperature T_K and power of incident radiation P_0 :

$$P_0 \approx \frac{2\pi \Theta(T_K)}{\mu_\omega(T_K)}. \quad (5)$$

The function $P_0(T_K)$ has a minimum (Fig. 7). It occurs at a temperature T_m that is much lower than the temperature at which absorption attains a maximum, i.e., a near-total single ionization of atoms takes place. When $P_0 < P_{\text{min}}$, steady-state regime is nonexistent. States for which $P_0 > P_{\text{min}}$ but $T < T_m$ are unstable: If the plasma temperature increases at random, much less

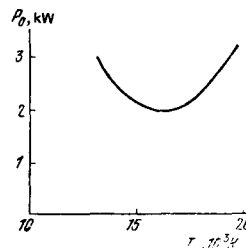


FIG. 7. Dependence of power of a spherically-symmetric converging beam on the maximum temperature of a plasma maintained in a stationary position, obtained by means of simple arguments. Air, $p = 1$ atm; beam, CO_2 laser.

power than in fact is sufficient to maintain the plasma. The heating will begin which will cause a transition into a state that corresponds to the same power, but not the temperature ($T > T_m$). This state is stable. The quantity

$$P_t \equiv P_{\min} \approx \frac{2\pi\Theta(T_m)}{l_{\omega \max}} \quad (6)$$

is the least, threshold power that is capable of maintaining a discharge. To reiterate, temperature at the center of a transparent optical discharge is close to a temperature of the total single ionization and the absorption maximum of laser radiation.

A formula of the type shown in Eq. (6) (with a slightly different numerical coefficient) was obtained in Ref. 23. In the proof above we have strictly followed a general line of reasoning which yields an approximate value of the plasma temperature in any stable discharge as a function of power, current strength, etc.,^{1,24,25} which underscores the uniqueness of all discharges of this kind. The existence of a threshold and the stability-instability of states are also typical situations.

The exact solutions which describe a steady-state optical discharge in the idealized model under consideration—a spherically-symmetrical regime which disallows radiative losses—are as follows:

$$\left. \begin{aligned} \frac{1}{r^2} \frac{d}{dr} r^2 \frac{d\Theta}{dr} + \frac{\mu_{\omega} P}{4\pi r^2} = 0, \quad \rho = \begin{cases} r & \text{at } r \geq \rho_0, \\ \rho_0 & \text{at } r \leq \rho_0, \end{cases} \\ \frac{dP}{dr} = \mu_{\omega}(\Theta) P, \quad \Theta = \Theta(T), \end{aligned} \right\} \quad (7)$$

where $P(r)$ is the radiation power at radius r , and S_0 is the "focal radius" that must be used to limit beam convergence in order to avoid infinite concentration of energy at the center. At $r = \infty$, $P = P_0$ and $\Theta = 0$; at $r = 0$, Θ is finite. Approximate solutions may be found for the equations, using a common simplification used in the theory of stable discharges— $\mu_{\omega} = 0$ at $T < T_0$, $r > r_0$ and $\mu_{\omega} = \text{const}$ at $T > T_0$, $r < r_0$ —which corresponds to the channel model of an arc, the "metallic cylinder" model for a rf inductive discharge, etc.^{1,20} (it is also assumed that $r_0 \gg S_0$).

In the case of a transparent plasma $\mu_{\omega} r_0 \ll 1$, both functions, $P_0(r_0)$ and $P_0(\Theta_k)$, have minima (for r_t, Θ_t); states with $r_0 < r_t, \Theta_k < \Theta_t$ are unstable. P_{\min} itself is close to Eq. (6). The minimum power corresponds to the plasma radius $r_t = \sqrt{(4/3)\rho_0 l_{\omega}}$, where $l_{\omega} = \mu_{\omega}^{-1}$ is the absorption length of light. In the preceding, simpler treatment, the radius r_0 fell out of the equations. It is now clear: The plasma radius is characterized also by a small quantity—the focal radius ρ_0 —which did not enter into these calculations.

In order to maintain a discharge in free air by means of a CO₂-laser radiation, power not less than $P_t \approx 2\text{ kW}$ is required, according to Eq. (6). The plasma temperature in this case is $T_m \approx 17,000\text{ K}$, $\Theta_m \approx 0.3\text{ kW/cm}$ and $\mu_{\omega \max} \approx 0.8\text{ cm}^{-1}$. For a typical value of $\rho_0 \sim 10^{-2}\text{ cm}$, absorbing region radius $r_t \approx 0.1\text{ cm}$. Figure 8 shows the results of the numerical solution of Eq. (7) for free air.⁴⁾ Two solutions are obtained for each value of P_0 . The solution for which the temperature at the cen-

⁴⁾ The solution was obtained by N. N. Magretova.

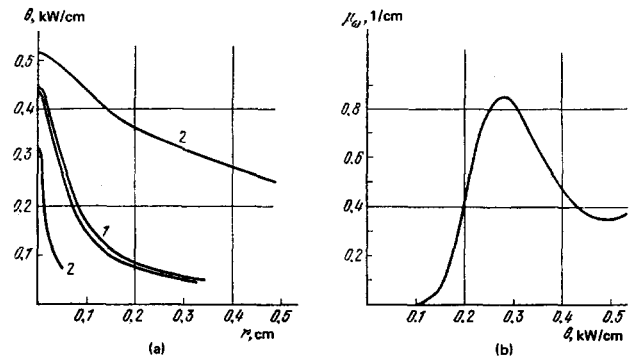


FIG. 8. Results of numerical solution of a spherically-symmetrical problem of plasma maintenance in free air by CO₂-laser radiation. (a) Radial distribution of thermal flux potential (lower curves 1 and 2 correspond to unstable solutions, upper curves—stable; curves 1 refer to a power $P_0 = 3.9\text{ kW}$ which is almost equivalent to threshold; curves 2— $P_0 = 4.5\text{ kW}$); (b) coefficient of absorption of radiation $\mu_{\omega}(\Theta)$ used in calculation.

ter is lower and the dimensions of a heated region smaller, corresponds to the unstable state. When $P_0 = P_t$, both equations degenerate into one. When $P_0 < P_t$, solutions which satisfy the foregoing boundary conditions are nonexistent. The value of $P_t = 3.9\text{ kW}$ agrees generally with results of a simpler estimate Eq. (6). Dimensions of a highly-heated region are also in agreement with the estimate.

(c) Why an unusually high temperature is obtained in an optical discharge

The temperature of arcs at the atmospheric pressure is normally 6000–9000 K, in rf discharges 8,000–10,000 K, and in microwave discharges 4,000–6,000 K. In the optical range, as we have just estimated and as is evident from experiment (see below), the temperature attains 20,000 K. This is associated partly with the fact that in an optical discharge very high fluxes, of the order of 10 kW/cm^2 are incident on a plasma surface $S \sim P_t/4\pi r_t^2$, which exceed the electromagnetic energy fluxes in other discharges ten- and hundredfold. However, the original cause of this is the fact that a plasma produced in a discharge at atmospheric pressure is transparent to optical radiation.

At lower frequencies, the field energy is well absorbed even in the case of a relatively weak ionization, i.e., at a relatively low temperature. Conversely, the field fails to penetrate a strongly ionized plasma, and thus impairs the conditions for a release of energy which subsequently occurs in a thin surface layer only. Because weakly-ionized gas fails to absorb the light at optical frequencies $\mu_{\omega} \sim \omega^2$ and the best dissipation occurs when the entire supply of electrons is consumed, i.e., at a full single ionization of atoms. The corresponding preheating of a plasma is unimpeded by the opacity which the field encounters.

If the plasma is opaque to laser radiation, the temperature in an optical discharge is as different from the fully-ionized temperature as it is also in other discharges. To show this, we shall consider a hypothetical spherically-symmetrical regime, but we shall al-

low for absorption of the converging radiation of a power P_0 by a plasma over a length $l_\omega = \mu_\omega^{-1}$ that is small compared to the radius of an absorbing sphere $\Theta = P_0 / 4\pi r$; $P_0 = 4\pi r_0 \Theta_0$. The radiation fails to penetrate the region $0 < r \leq r_0 - l_\omega$. In that region, according to the equation of thermal conductivity Eq. (7), $\Theta = \text{const} = \Theta_K$. The total temperature difference $\Delta T = T_K - T_0$ and the potential difference $\Delta\Theta$ are applied to a comparatively thin absorbing layer, and the release of energy from inside is determined by an approximate relation $P_0 \approx 4\pi r^2 \Delta\Theta / l_\omega$. Now, $\Delta\Theta / \Theta_0 \approx l_\omega / r_0 \ll 1$ and $\Delta T / T_K \ll 1$.

However, if a relatively small rise in the temperature causes a change in the absorption from weak to strong, this means that an increase in the level of ionization is sufficiently sharp in this case. This is possible only in a region characterized by reasonably low ionization levels and temperatures, where $n_e \sim \exp(-I/2kT)$ and $I/2kT \gg 1$. The electron density increases e -fold in the temperature interval $\Delta T \approx (2kT/I)T \ll T$ which is approximate and may be considered to be $T_K - T_0$. This is the case also in the microwave, rf and arc discharges.^{20,25} In the case of an opaque optical discharge considered above, temperature in the central region T_K varies slowly, logarithmically with increasing power P_0 , and it decreases while the plasma radius r_0 increases. Thus, in the case of spherically-symmetric convergence of radiation with $P_0 = 13$ kW in air at the atmospheric pressure, we would obtain $T_K \approx 14,000$ K, $\mu_\omega \approx 0.6$ cm⁻¹, $r_0 = 6.3$ cm, $\mu_\omega r_0 = 3.8$, and $S = 26$ W/cm². At $P_0 = 37.5$ kW, $T_K \approx 12,500$ K, $\mu_\omega \approx 0.3$ cm⁻¹, $r_0 \approx 20$ cm, $\mu_\omega r_0 \approx 6$ and $S = 7.5$ W/cm². Of course, these examples are very remote from conditions of actual experiments; they are cited for the sole purpose of illustrating the considerations expressed above. However, focusing a beam whose power is noticeably above threshold does, in fact, cause displacement of a plasma from the focus toward the beam, increase in the size of a plasma and, most likely, decrease in the temperature.

The inordinately high temperature is a unique property of the continuous optical discharge at a relatively low pressure, which opens great possibilities for using it as a high-temperature source, all the more considering that a discharge can burn with stability over long periods of time, of the order of hours. Blinding white light emanates from the optical discharge plasma which cannot be viewed long without dark glasses.

(d) Measurement of temperatures and thresholds

When the first experiments were planned, CO₂ laser power did not exceed 150 W. However, Eq. (6) suggests conditions under which power requirements are reduced. A discharge must be produced in a heavy monatomic gas in which energy release due to thermal conduction is small at elevated pressures at which the absorption of laser radiation is stronger. A continuous optical discharge was ignited for the first time in xenon under a pressure of several atmospheres.²² Subsequently, more powerful lasers were used to produce a plasma in several gases at different pressures, including atmospheric.²⁶⁻³⁴

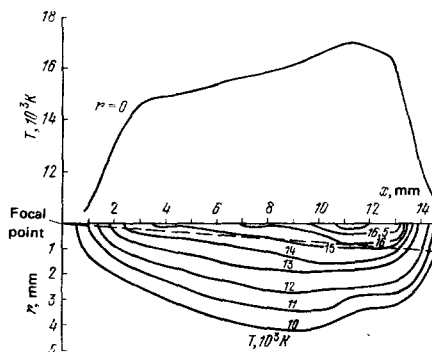


Fig. 9. Space-dependent temperature distributions (isotherms) in a continuous optical discharge in atmospheric-pressure air (Ref. 30). CO₂ laser power, 6 kW. Beam travels from right to left. Effective boundary of converging light channel shown as a dashed line. Curve above horizontal axis—temperature distribution along beam axis.

A discharge in free air was obtained in Ref. 29 and was investigated in detail in Refs. 30 and 31 by means of 6-kW CO₂ lasers. Experiments²⁹ have confirmed the theoretical predictions.²³ The experimental threshold was approximately 2 kW. An estimate of the maximum plasma temperature was also confirmed. According to measurements near the center $T \approx 17,000$ K³⁰; further away from the center $T \approx 15,000$ K was recorded.³¹ Figure 9 shows a series of isotherms—two-dimensional discharge plasma temperature distributions.³⁰ The laser beam converges at a small angle as a result of focusing by a $f = 15$ cm lens. The temperature was measured by spectroscopic methods: emission in the continuum in a narrow wavelength interval near $\lambda = 5125$ Å, and emission in the atomic and ionic lines of nitrogen. The plasma center was shifted from the focus toward the beam by 1.1 cm. Very similar isotherms were obtained in Ref. 31, where the spatial distribution of n_e was measured by means of the two-wavelength laser interferometry; the temperature was calculated from n_e under the assumption of a plasma stability.

In the first investigation,²⁶ the electron density in argon was measured at $p = 2$ atm from the Stark broadening of the H β hydrogen line, $n_e \approx 3.5 \times 10^{17}$ cm⁻³, which corresponds to the temperature of 23,000 K at equilibrium. Evidently, this figure appears to be inflated; subsequent and more detailed measurements of the absolute line intensity of the 4806 Å Ar II ion under similar conditions have yielded 18,000 K at the plasma center.²⁸ In xenon at 2 atm the maximum temperature is lower, 14,000 K (measured from the absolute line intensity of the 5292 Å Xe II ion).³² This is natural: the ionization potential in xenon is smaller than in argon. In hydrogen, under 6-atm pressure and 1-kW laser power, the maximum temperature measured from the absolute intensity of the continuum at 2500 Å, was 21,000 K.³⁴ In nitrogen, under 2 atm and 0.9 kW, the temperature at the center of the plasma and measured from the intensity of the 3995 Å N II line, was $T = 22,000$ K.³⁴ In other experiments,^{28,32,34} the radial temperature profiles were taken at cross-sections where the radius of a plasma configuration was maximum: the plasma center was shifted from focus toward the beam by several mm.

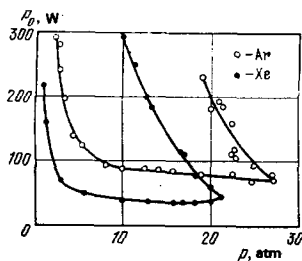


FIG. 10. Threshold powers required to maintain continuous optical discharge in monatomic gases (lower curves). Also shown, upper boundaries of discharge (upper curves) (Ref. 26).

The radial size of a plasma at half temperature level was 1–2 mm.

Figures 10 and 11 show the results of measurements of the threshold power at various pressures in atomic²⁶ and molecular³⁴ gases. The lower curves show minimum powers that are sufficient to maintain a steady-state discharge and are characterized by a sharp power drop at comparatively low pressures, and ending in a considerably weaker function $P_t(p)$ (see below concerning the sense of the upper curves). The sharp drop is characteristic of a process in which the energy in a plasma is released through thermal conduction: according to Eq. (6), $P_t \sim p^{-2}$, if $\mu_{\omega \max}$ increases with pressure as p^2 . Subsequent increases in the pressure result in a gradual change in the dominant mechanism of energy losses. A progressively larger role is played by thermal radiation losses. As long as a plasma remains transparent to thermal radiation, these losses increase, roughly speaking, as p^2 , while thermal conduction losses remain weakly dependent on the pressure. Thresholds are significantly higher in molecular gases than in monatomic: In the high-temperature region, molecules dissociate into atoms which, while diffusing into a region of lower temperatures, recombine there with a release of the binding energy. As a result of this, the resulting thermal conduction and thermal flux potential $\Theta(T_m)$, which is proportional to the threshold power, increase substantially.

(e) Radiative losses

It is well known that at pressures of the order of 10 atm radiative energy losses in a discharge plasma overshadow thermal conduction losses. This underlies the operation of high-pressure xenon arc lamps in which up to 80–90% of the Joule heat is converted into

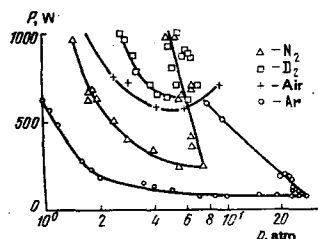


FIG. 11. Threshold powers required to maintain continuous optical discharge in molecular gases (lower curves). Upper boundaries of discharge also shown (Ref. 34).

thermal radiation. Naturally, the same thing also occurs in the optical discharge. The elementary concept of a plasma radiation may be obtained from the Unsöld-Kramers theory (see Ref. 35). At temperatures, corresponding to the first ionization, the energy released in a continuous spectrum is

$$\Phi = \frac{32\pi}{3} \left(\frac{2\pi kT}{3m} \right)^{1/2} \frac{e^2 n_e n_{n_+}}{mc^3 h} \left(1 + \frac{h\nu_g}{kT} \right) = \frac{7.6 P_{\text{atm}}^2 x_e^2}{(T[K]/404)^{3/2}} \left(1 + \frac{h\nu_g}{kT} \right) \text{ kW/cm}^2, \quad (8)$$

where x_e is the electron mole fraction. The first term—proportional to the element in parentheses—describes bremsstrahlung and the second—the principal—describes photorecombination radiation; $h\nu_g$ is the binding energy of the lower excited level of an atom. The ground-level electron captures, at which $h\nu > I$ photons are emitted, are not included in Eq. (8). These photons are strongly absorbed by unexcited atoms, and hardly leave the place of their origin.

The energy balance of an optical discharge in the case of predominant radiative losses are expressed by the equation

$$S\mu_{\omega} = \Phi. \quad (9)$$

Inasmuch as both μ_{ω} and Φ are identically proportional to $n_e n_{n_+}$, the intensity of laser radiation S that is required to maintain a plasma at a certain temperature, depends weakly on the pressure, a fact which qualitatively explains the sharp reduction in the dependence of P_t on p at $p \geq 5$ atm. We note that after the onset of the second ionization, μ_{ω} and Φ are augmented by terms proportional to $Z^2 n_e n_{n_{++}}$, where $Z=2$ and $n_{n_{++}}$ is the charge and density of doubly-ionized atoms.

Radiative losses may play an important role also at atmospheric pressure, but at elevated laser powers, at which the plasma dimensions increase. Moreover, energy losses due to thermal conduction are reduced by virtue of the reduced temperature gradients. Thus, in an optical discharge in free air and at $T \approx 15,000$ – $18,000$ K, the emittance—calculated by combining different data—is 40–60 kW/cm² and the radiative losses are comparable to thermal conduction losses when the highly-heated region is of the order of 1 mm and up.^{1,23} The role of radiative losses in this case may be judged indirectly by comparing the energy yield and losses due to thermal conduction, calculated from the experimental isotherms shown in Fig. 9. This shows that approximately 2/3 of energy released from the central portion of a plasma is carried away by thermal conduction, i.e., 1/3 is attributed to radiative losses.

Equation (8) describes emission in the continuum only. Meanwhile, according to extensive data, much greater energy may be emitted in the spectral lines. Line emission is also proportional to $n_e n_{n_+}$, because excited atom densities are proportional to it.³⁵ An approximate formula for the total radiation was proposed on the basis of certain theoretical considerations,²⁸ which can be used to generalize Eq. (8) by way of including the spectral line contribution [which we shall designate $\Phi_1(T, p)$]. The main difference between Φ_1 and Eq. (8) is the replacement of the term $(1 + h\nu_g/kT)$ by $\exp(h\nu'_g/kT)$, where $h\nu'_g$ is the bonding energy of the lower levels that are taken into consideration. As an example of the lat-

ter, excited states higher than the lowest are used in inert gases (in argon, for example, $h\nu'_g = 2.85$ eV as opposed to $h\nu_g = 4.3$ eV). The empirical choice of $h\nu'_g$ provides the best agreement with experimental results for the emittance of an optical discharge plasma.^{28,32} These experiments have shown that in argon at $p \approx 6-10$ atm and $P_0 = 600$ W, nearly one half of the incident laser energy, i.e., a large portion of absorbed energy, is emitted by the plasma. When $P_0 - P_t \approx 100$ W, and the plasma size shrinks, the relative importance of radiative losses is grossly reduced.

(f) Upper limits of power

As was shown in Ref. 26, a discharge is extinguished at high pressures if the laser power exceeds a certain upper limit which depends on the pressure and, generally speaking, it fails to burn above a certain p (see Fig. 10). It was first believed that this was associated basically with emergence of a plasma from the beam induced by the Archimedean force. However, this effect was later explained in terms of radiative losses.²⁸

The function $S(T) = \Phi_1(T) / \mu_\omega(T)$ —defined by Eq. (9)—has a minimum: in argon at $10.6 \mu\text{m}$, $S_{\text{min}} \approx 6 \text{ kW/cm}^2$ at $T_1 \approx 12,700$ K. If $S < S_{\text{min}}$, the plasma breaks up.⁵⁾ States with $T < T_1$ are, as always, unstable. When moving away from the focus after an initial ignition, the plasma front propagates along a path $R = R_1$ inside an expanding light cone to a cross-section where $S = P_0 / R^2 \Omega = S_{\text{min}}$ (Ω is a solid aperture angle of the cone), and it stops there. For example, in argon at $p = 10$ atm and $P_0 = 600$ W, $\Omega = 0.45$ rad and $R_1 = 0.4$ cm; both values agree with experiment.

In a steady state, the laser radiation propagates through the plasma towards the focus; its intensity tends to increase as a result of beam convergence, and to decrease due to absorption. The first process is independent of pressure, and the second increases with increasing p . This means that for each value of power P_0 , beginning with some value p , the second process is more likely to occur and the plasma intensity should decrease with depth with respect to S_{min} at the leading edge. But, when $S < S_{\text{min}}$, steady-state maintenance of a plasma is impossible. If the power is increased for a given p , R_1 increases, the effect of the geometric factor is reduced and, at some value of P_0 , it yields to absorption; once more $S < S_{\text{min}}$ in the plasma. This explains the upper limit of existence of a discharge.

5. PROPAGATION OF OPTICAL DISCHARGES

(a) Propagation mechanisms and an analogy with burning

All discharges tend to propagate. Mechanisms exist for the energy transfer from a discharge plasma to the

⁵⁾ It is conceivable that such a serious property—specific to many discharges—as the existence of a minimum flux density of the electromagnetic energy that is required to maintain a plasma, depends on a choice of a specific radiative loss function in Eq. (8), for example, $S(T) = \Phi(T) / \mu_\omega(T)$ behaves monotonically and has no minimum. In fact, when losses due to thermal conduction are taken into account, Eq. (9) is generalized: $S\mu_\omega = \Phi + a\Theta$, where a is some coefficient. The function $S = (\Phi + a\Theta) / \mu_\omega$ has a minimum, only if $\mu_\omega(T)$ has a maximum, a fact that is known already.

surrounding layers of cold gas, which enhances ionization. If a newly ionized layer lies in an external field, the field energy begins to dissipate in it and the layer is enveloped in a discharge. The same happens later to subsequent layers, etc.

The plasma front which bounds a region enveloped by discharge, moves along the gas. The discharge remains stationary and it appears to be static under the conditions whereby its motion is inhibited by walls, or if the field intensity beyond its limits is insufficient to maintain a plasma.

Different mechanisms of energy transfer and stages of ionization, from the discharge plasma to adjacent cold layers, are possible: shock wave, thermal conduction, radiative heat transfer; ionization is enhanced by diffusion of resonant radiation, electron diffusion.

Discharge propagation effects (in certain cases termed "ionization waves") were observed and experimentally studied under the most diverse conditions.¹ The most frequent example of this effect is a process occurring in plasmotrons, where the discharge remains stationary in space and a gas flows through it. This has little fundamental value, and it reduces to a mere question concerning the choice of a coordinate system to be used in observations. The propagation mechanism in the stable plasma generators is normally thermal conduction of heat, followed by thermal ionization of cold gas masses.

The above mechanism has much in common with burning in a gas torch, where a combustible mixture enters a plasma in a steady-state continuous flow, while the plasma remains stationary. Generally speaking, there is a far-reaching analogy between the processes of propagation of discharges and flame. The analogy is contained in the same strong temperature dependence of the rate of chemical reaction and the rate of dissipation of field energy which is proportional to the degree of ionization (or its square) of a gas. Both functions follow the Boltzmann law $\exp(-\text{const}/kT)$. The gas ionization temperature introduced above corresponds to the ignition point of a fuel below which a chemical reaction practically cannot proceed. The processes of energy release, energy transfer from the heated matter (combustion products, discharge plasma) to cold and the heating of the latter to the ignition point, ionization, motion of the flame and discharge fronts, all occur identically. The difference lies only in the source of energy: either the chemical energy contained in the matter itself, or the field energy supplied from outside.

(b) "Light detonation"

Motion of a plasma front in a laser field, an event which belongs to a class of processes dealing with discharge propagation, was discovered during the original investigation of the laser spark. The boundary of the optical discharge plasma moves toward the laser beam, from the focal point, with a velocity of the order of 100 km/s. The mechanism of discharge propagation in this case is a shock wave that heats the gas to a very high temperature at which the gas undergoes strong

ionization. The effect is similar to a process involving detonation of explosives, in which the latter are heated to the ignition point by a strong shock wave that, in turn, is propelled by pressure generated by a rapidly burning explosive. This phenomenon was thus interpreted as "optical detonation." The mechanism involved, is uncharacteristic of discharges and, evidently, it occurs naturally at optical frequencies only. In order to produce a rapid supersonic motion of the "detonation" front, very large energy fluxes are required, and at all other frequencies the corresponding electric field intensities are above the breakdown threshold. Therefore, in any other field but optical, a gas would break down before the occurrence of the "detonation" wave. Since our goal is to demonstrate the common features that unify optical discharges with all others, we shall not dwell here on the subject of "optical detonation."⁶⁾

(c) "Slow burn" regime

The "slow burn" process of propagation of a stable optical discharge—based on the mechanism of thermal conduction—is similar to the slow (subsonic) burning of combustible materials. In contrast "detonation," processes of this type are observed in all fields without exception. In the optical range, this effect was observed for the first time in Ref. 38. A millisecond pulse from a neodymium-glass laser, containing an energy of 1,000 J, was focused in air by a long-focus lens with $f=50$ cm. The peak power was 1 MW and the light intensity at the focus ~ 10 MW/cm². The latter is two orders of magnitude lower than required for breakdown; however, while an initial plasma was produced in the focal region by means of an ordinary breakdown between electrodes, plasma fronts were traveling along the beam in both directions from the focus (both directions, since the plasma is highly transparent to radiation from a neodymium-glass laser). The velocities were small (of the order of 10 m/s) as was also temperature, in contrast to high "detonation" values ($v \sim 100$ km/s, $T \sim 10^6$ K). The effect was interpreted as "slow burning."³⁸⁾

The theory of a thermal conduction regime was developed in Refs. 1, 21 and 23. In an idealized one-dimensional formulation, the steady-state regime of propagation of the "optical burning" wave that is traveling toward a parallel optical beam by way of a parallel optical beam by way of a thermal conduction mechanism and is maintained by the beam energy, may be described in a system of coordinates associated with the front (see Fig. 12) by the following equations:

$$\rho_0 v c_p \frac{dT}{dx} = \frac{d}{dx} \bar{\lambda} \frac{dT}{dx} - A \frac{\Theta}{R^2} + S \mu_\omega, \quad (10)$$

$$\frac{dS}{dx} = -\mu_\omega S; \quad (11)$$

where c_p is the specific heat at constant pressure, ρ_0 is the density of cold gas, v is velocity at which the

⁶⁾ For details, see Ref. 1. We shall point out new experiments in which a light detonation wave was forced out of a target³⁶ and into the volume of a free gas due to breakdown of another laser.³⁷

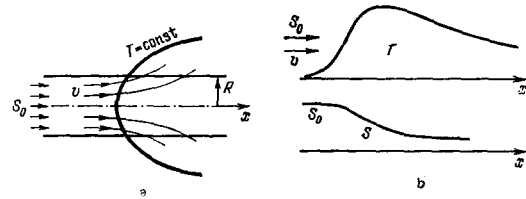


FIG. 12. Diagram of light burning wave in a parallel beam. (a) Qualitative pattern of heat flow and gas expansion. Isotherm and flow lines are shown; (b) Idealized one-dimensional regime [$T(x)$ and $S(x)$ distributions are shown].

gas enters a discharge and is equal to the velocity of propagation of a front in the gas. The mass flow at a given point x is constant and equals $\rho_0 v$; density ρ is related to temperature under the condition of constant pressure $p \sim \rho T \approx \text{const}$. The term $A\Theta/R^2$, which substitutes for the radial portion of the Laplacian Θ , allow in an approximate way for a release of energy due to thermal conduction through a lateral boundary of the optical channel (plasma energy losses). The coefficient $A \approx 3$ is determined by the radial temperature profile which falls from the axis to periphery.

In front of the wave, at $x = -\infty$ and $T=0$, $S=S_0 = P_0/\pi R^2$, where P_0 is the incident beam power. After a beam is completely absorbed, the gas cools off as a result of losses, such that at $x = \infty$, $T=0$. The solution of a second-order equation for T is subject to two boundary conditions. However, one of the arbitrary constants is not subject to definition due to the arbitrariness with which the origin of the coordinates x was picked. Consequently, one of the boundary conditions is "superfluous." This provides an opportunity in the course of seeking a solution to determine the unknown parameter, the "normal" (in analogy with the theory of combustion) discharge propagation velocity v . Similarly formulated, although allowing for real special features of the geometry and field, are the problems concerning the propagation of rf and microwave discharges,¹ and also of a flame.

In those cases that are important in practice, where the optical absorption length in the fundamental energy yield region, i.e., at the highest temperatures in the wave, $l_\omega = 1/\mu_\omega$, clearly exceeds the diameter of the light channel $2R$, the problem is simplified. This occurs when the wave motion is induced by radiation from a neodymium-glass laser, and, in the case of CO₂-laser radiation, at the atmospheric pressure and radii R , not exceeding one-two mm (in air, $l_{\omega \text{ min}} \approx 1.2$ cm). Under these conditions, energy expanded in advancing a wave is, basically, the energy which is absorbed at a distance of the order of a diameter from the leading front of a plasma. The energy absorbed far from the front, is wasted through a side boundary of the channel. In the active part of the wave, the flux S is barely weakened. In that part alone and considering it a "wave," Eq. (11) may be omitted, having assumed $S \approx \text{const} = S_0$ and having set a boundary condition behind the "wave" at $x = -\infty$, defined as $dT/dx = 0$. The final plasma temperature, moreover, is automatically determined by the balance equation behind the wave $S_0 \mu_\omega(T) = A\Theta(T)/R^2$.

Equation (10) may be linearized with respect to Θ , having assumed $c_p/\lambda = \text{const}$ and $\mu_\omega = 0$ at $\Theta \leq \Theta_0$, and $\mu_\omega = \text{const}$ at $\Theta \geq \Theta_0$ (see Section 4), and it is readily and accurately solved. The wave maintenance threshold corresponds to a limit $v \rightarrow 0$ in the solution. In the case of purely conductive losses, the threshold is characterized by the total power $P_t = S_t \pi R^2$, as also in a spherical case (Section 4). Formula of the type of Eq. (6) is obtained for P_t and it contains an additional coefficient of the order of unity. The maximum temperature T_K also differs little from the temperature of the total single ionization T_m ($T_K > T_m$). In the case of CO_2 -laser radiation and $R \leq 0.05$ cm, when losses are due to strictly thermal conduction, threshold in the free air is $P_t \approx 4$ kW, which exceeds the maintenance threshold for a static continuous optical discharge in a well-focused beam. As the channel radius increases, radiative losses become appreciable and the threshold is now characterized not simply by the power but the light intensity and radius R . At $R = 0.15$ cm, calculations yield $S_t \approx 100$ kW/cm² and $P_t \approx 7$ kW.²³ The plasma temperature in a wave is, as before, $T_K \approx 17,000$ K. The calculated threshold of $P_t = 920$ kW, for a neodymium-glass laser beam with $S_t \approx 1.3 \times 10^4$ kW/cm², is in a good agreement with experimental results.³⁸

The propagation velocity of the "light burning" wave in a gas is greater, the greater the intensity of radiation which maintains it. At powers considerably exceeding threshold, velocity is characterized by the following expression

$$v \approx \frac{\lambda}{\rho_0 c_p} \sqrt{\frac{S_t \mu_\omega}{\Theta_0}}, \quad (12)$$

which corresponds to the well-known Zel'dovich formula for flame propagation. Calculations, based on a more exact solution of Eq. (10), show that the velocity v is of the order of 1 m/s, a value which is characteristic for the slow thermal-conductance mechanism of wave propagation. Meanwhile, experimental values are, as a rule, an order of magnitude higher.

The source of discrepancy is the fact that in an experiment the plasma wave front is observed, as a rule, to propagate in a cold gas which is moving in the same direction, not unlike the case in which a flame propagates in a tube from the closed end (this explanation was offered in Ref. 38). Actually, a discharge plasma, heated to a high temperature, undergoes thermal expansion and, like a piston, pushes the ambient cold gas, including those layers which lie ahead of the front. The velocity with which the cold gas is moving in the direction of propagation of the front is on a par with the rate of the steady-state motion of a plasma in a coordinate system in which a wave is at rest: $v_K = v \rho_0 / \rho_K$ (ρ_K is the plasma density; $\rho_0 / \rho_K \approx T_K / T_{\text{initial}}$). The latter is tenfold greater than the normal propagation velocity v , such that in an experiment not v , but actually a velocity of the order of v_K is recorded.

The problem³⁹ linearized with respect to Θ , was generalized by way of allowing for two-dimensional thermal-conductance effects: The first two terms in the right-hand side of Eq. (10) are written precisely in the form of the Laplacian Θ . Added to it is also a lin-

earized term for the radiative losses $\Phi = \text{const} \Theta$. The light channel is considered as if it were placed inside a cooled tube with a radius $R_1 > R$, where $\Theta = 0$ at the walls. A solution $\Theta(x, r)$ is sought in the form of a series by the method of separation of variables. Numerical calculations were carried out for the free air. An isotherm plot obtained is very similar to the one obtained experimentally.³⁰ A good agreement is observed between the effective constant of radial losses A in Eq. (10), obtained in experiment, and an estimated value $A = 2.9$ used in Ref. 23.

A numerical calculation was carried out for an unstable motion of a wave from the ignition point—the focus—toward a converging beam.⁴⁰ The problem is formulated in a one-dimensional mode. The nonsteady-state equation of thermal conductance is expressed in the spherical coordinates to suit the conical beam geometry; the angular portion of the Laplacian Θ , as also the radial in Eq. (10), is replaced by the expression $A\Theta/R^2$, where now $R = r \tan \varphi$ is the instantaneous radius of cross-section of the conical channel; 2φ is the cone aperture angle. Calculations were made for argon at very high pressures (5–50 atm) and, therefore, the radiative losses included in the equation play an important role. The plasma front travels along and slows down an expanding light channel, and then stops. The stopping point and the temperature of a static discharge are closer to S_{min} (see end of Section 4), the higher the pressure and the greater the power, i.e., the greater the relative role of radiative losses.

(d) Experiments

Subsonic propagation of a discharge in the light channel of a laser beam was investigated experimentally in a number of works.^{26,31,38,41–43} We have already discussed the first experiment.³⁸ In subsequent experiments,⁴¹ carried out in a wide interval of pressures (17–80 atm), measurements were made of thresholds at which waves occur and velocities with which they move in argon, while maintained by focused, spikeless millisecond pulses from a ruby laser. The threshold decreased with increasing pressure, sharply at first, slowly later, a fact that may be explained by losses due to thermal conduction being replaced by radiative losses. The velocities were of the order of tens of m/s.

The process of wave propagation from the focus always precedes the establishment of a static continuous optical discharge.^{26,31}

In the experiments, 400-kW CO_2 gas-dynamic laser beam 10 cm in diameter was focused on a target by an $f = 55$ cm mirror to a spot 0.5 cm in diameter.⁴³ The beam intensity at the focus was $S \approx 1.2$ MW/cm². A discharge wave was set into motion in air from the target toward the beam, which covered a distance of approximately 10 cm during a laser pulse lasting 4 ms. The wave front velocities were of the order of 20–50 m/s. By comparing such high experimental front velocities with normal purely thermal-conduction propagation velocities calculated in Ref. 23 (~ 1 m/s), the authors perceived a clear contradiction with the theory,²³ and on

this basis concluded that the leading role in the wave propagation is played by radiative heat transfer.

Without rejecting the possibility of a radiative mechanism being responsible (see below), we should point out that similar comparisons and arguments cannot be acknowledged as being correct. In the case of burning "from the closed end"—and, in some experiments, a solid target which induces burning was used as a "tube end-piece"—the velocity of a wave in the space may several tenfold exceed the thermal-conduction velocity of propagation through the bulk (see above), i.e., it may be exactly of the order of observed velocity. This case has received attention also in Ref. 44, which is dedicated to a mechanism of radiative heat transfer, and a comparison of calculations with experiment.⁴³ A series of time-lapse photographs of the process, occurring under the conditions similar to those in Ref. 43, were taken.⁴²

It is worth pointing out that in the technological processes involving lasers, continuous optical discharges frequently occur at the surfaces being processed by sufficiently powerful cw CO₂ lasers. In this case, the effect is harmful: By absorbing the laser radiation, the plasma screens the surface and impedes the intended coupling of energy to the target.

(e) Radiative heat transfer

The radiative regime of propagation of an optical discharge wave, in which the driving mechanism is radiative heat transfer, was analyzed in one of the first works dealing with the laser spark⁴⁵; it dealt with giant-pulse lasers for which the beam intensities were $S \approx 10^4$ – 10^6 MW/cm², the high temperatures behind the wave front were $T \approx 10^5$ – 10^6 K, and the propagation velocities were supersonic, as is the case with "detonation" (see also Ref. 1). In the range $S \approx 10^2$ – 10^3 kW/cm², which is typical for experiments in slow burning in a CO₂-laser beam, the radiative regime is also possible, although it is subsonic.

The difference between the latter case and the supersonic regime is basically quantitative. The subsonic process takes place at a constant pressure, not density. The heated plasma is considerably less dense than the cold gas; it is transparent and weakly radiative, its temperature is relatively low, $T \approx 20,000$ K, and the cold gas is transparent to the bulk of thermal radiation. The only radiation absorbed in it and involved in the heat transfer is the hard ultraviolet, which comprises a small portion of the entire emission spectrum. The cold air, for example, fully transmits the entire radiation with $\lambda \geq 1860$ Å.

The high level of plasma transparency to natural thermal radiation underscores a special property of the radiative regime: dependence of its effectiveness on the light channel diameter. Since the plasma emits volumetrically, and the lattice occurs at relatively low pressures—specifically, atmospheric pressure—wave advancement requires energy that is emitted by a plasma layer with an axial length of the order of the diameter. At a distant point, the wavefront cross-section

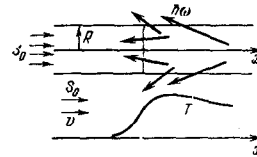


FIG. 13. Diagram of a wave driven by radiative heat transfer mechanism.

is observable under a narrow solid angle, and the majority of photons produced there are emitted outside the region before the front, which front is subjected to heating (see Fig. 13). According to estimates for free air,²³ radiative heat transfer yields to thermal conduction in the case of light channel diameters less than several mm. The radiative mechanism takes over only in the case of diameters of the order of 1 cm and up.

The radiative heat transfer mechanism has been considered as a two-group approximation.^{46,47} The entire spectrum of thermal radiation may be divided into two parts: hard, with $\lambda < 1130$ Å, $\hbar\omega > 10.9$ eV, for which a common large absorption coefficient which is independent of λ is assumed, and soft, with $\lambda > 1130$ Å, characterized by weak absorption. It is considered that the hard radiation is in a local thermodynamic equilibrium with the plasma, and a radiative heat transfer approximation, which augments the thermal conductivity of material, is assumed to be its means of transport. The soft radiation takes part in only bulk radiative losses. The problem is reduced to a thermally-conductive wave with the total heat transfer coefficient that is strongly temperature dependent. The calculated radiative heat transfer⁴⁷ leads to relatively high wave propagation velocities, of the order of tens of m/s which were recorded experimentally.⁴³ However, we believe that the use of the radiative heat transfer approximation in the case of light channels with diameters of 0.25–0.5 cm, considered by these authors, is unjustified. At the temperature of the radiant plasma in the range 15,000–20,000°C, the free path of hard radiation responsible for the heat transfer is 0.7–1.0 cm, i.e., it is several times greater than the diameter which renders the use of the radiative heat transfer approximation unacceptable. Actually, the nature of emission is volumetric and the effect of radiative heat transfer is significantly weakened. The resultant wave velocities are lower.

In the highly detailed calculations⁴⁴ analysis of radiation transport calls for a division of the entire spectrum into nineteen frequency groups and the tables of spectral optical properties of air are used. International numerical methods have been developed for the self-consistent solution of the gas energy equation of the type of Eq. (10), which includes a radiative heat transfer term, and for the radiation transport equation. However, plane one-dimensional regime is considered, without allowing for the radial limitation of the light channel. Consequently, solution is applicable to only sufficiently broad light beams with diameters of the order of 1 cm and up, as also stipulated by the authors. The propagation velocities are of the order of tens of m/s which, in general, agrees with the results

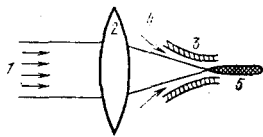


FIG. 14. Principal scheme of an optical plasmotron (Ref. 50). 1—laser beam; 2—lens; 3—nozzle; 4—gas flow; 5—plasma jet.

obtained in Ref. 43, although the channel diameter in the latter was somewhat smaller. Most probably, in these experiments the concurrent thermal conduction and radiative processes develop against the background of a rapid motion of a cold gas before the front, which is pushed by the expanding plasma ("burning from the closed end"). One-dimensional radiation waves, which propagate from a target at elevated beam intensities, together with the hydrodynamic motion were calculated numerically⁴⁸ and investigated experimentally.⁴⁹

6. OPTICAL PLASMATRON

(a) Experiments

It was noted in Section 4 that a plasmotron may be built, based on the principle of a continuous optical discharge, provided—as it is done for all other fields—cold gas is blown through the discharge. A free-air plasmotron would require very high powers: according to calculations discussed above, a minimum of 4 kW. However, smaller powers are sufficient in gases (monatomic) with a lower threshold. The corresponding experiment, carried out in argon by means of a 0.8-kW CO₂ laser, was described in Ref. 50. The beam was focused in the region of a nozzle through which argon was ejected in the same direction as the beam (Fig. 14). A jet of plasma, formed in the continuous optical discharge, flowed directly into the air. The radius of the brightly shining region was of the order of mm, and the length, approximately 3 cm.

The plasma in the optical discharge, which burns in a stationary gas, is always shifted from the focus toward the beam (Figs. 6 and 9). Investigation of a stationary discharge in a flow directed along the beam as shown in Fig. 14, showed that the greater the flow velocity v the closer the flow pushes the leading plasma

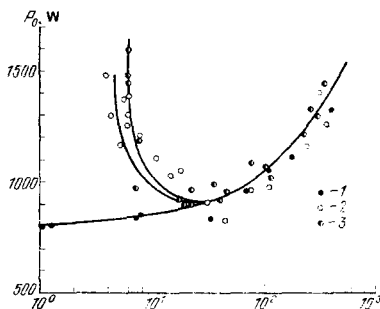


FIG. 15. CO₂ laser power required to maintain a stationary optical discharge in atmospheric-pressure argon flow as a function of flow velocity (Ref. 51). 1—radiation focused by $f = 10$ cm lens; 2— $f = 20$ cm; 3— $f = 40$ cm (abscissa represents velocity v in cm/s).

front to the focus.⁵¹ The discharge is "blown away" in both rf and microwave plasmotrons.¹ The laser power P_0 that is required to maintain steady-state burning depends, of course, on the flow velocity v . The latter is also the velocity of discharge propagation in a gas. When the CO₂-laser radiation is focused by short-focal lenses, in particular $f = 10$ cm, in argon at the atmospheric pressure, P_0 increases monotonously with increasing velocity from zero (Fig. 15). However, the function $P_0(v)$ ceases to be monotonic (as can be seen in Fig. 15) in near-parallel beams ($f = 20, 40$ cm); at velocities $v < 5-8$ cm/s and, all the more, in a stationary gas, a discharge generally fails to burn.⁷⁾

(b) Velocity limits of discharge burning

To explain the existence of a minimum propagation velocity for a discharge burning in the weakly-converging or parallel beams, it has been proposed⁵¹ to treat—in analogy with results presented in Ref. 52—the propagation velocity of the plasma front v as being proportional to the heat release gradient F kW/cm³ at a point $x = x_m$, where the plasma temperature $T(x)$ is at a maximum. The front moves along a gas in the direction of increasing F , and the gas flows through a discharge in the direction of decreasing F ; in this case, $v > 0$. Thus,

$$v \sim - \left(\frac{dF}{dx} \right)_m. \quad (13)$$

The light intensity S in a parallel beam decreases along the beam due to absorption, $F = \mu_\omega(T)S$ hence, $v \sim (\mu_\omega^2 S)_m > 0$.

If the beam is focused, S and F both concurrently increase along the beams as the latter converge. In the case of weak focusing, absorption predominates and $v > 0$; to hold a discharge stationary requires a flow in the opposite direction. When the focusing is sufficiently strong, compensation of the two effects is possible; hence, $(dF/dx)_m \sim (dS/dx)_m = 0$ and a discharge may burn in a stationary gas.

In the above considerations the dominant role is correctly attributed to the effect of absorption of light flux and a competition between light absorption and beam convergence, although the mechanism by which attenuation or intensification of the light flux affects the front velocity is unknown. Clearly, it is assumed, the latter is the same as the mechanism which gives rise to Eq. (13). However, this problem cannot be considered solved because Eq. (13) does not actually hold for the steady-state burning regime under consideration. Instead, it pertains only to a stage of non-steady-state motion of a plasma from an initial, strongly-symmetrical—with respect to a maximum point—distribution $T(x)$.⁸⁾

Without repeating the complex proof of Eq. (13) which

⁷⁾ Ignition of a discharge in standing free air also failed when an $f = 50$ cm lens was used for focusing.²⁹

⁸⁾ Displacement of a radially-symmetric dc arc column in the direction of incident microwave radiation that was parallel to the flux was considered.⁵²

was offered in Ref. 52 in the most general form, we shall track its behavior using a relatively simple example, of interest to us, involving a one-dimensional regime of an optical discharge wave in a parallel beam that is stationary in a system of coordinates where the plasma is quiescent. This regime is described by Eqs. (10) and (11). We shall proceed in Eq. (10) from T to Θ , assume $c_p/\lambda = \text{const}$, differentiate the equation with respect to x and refer it to a point where T is at maximum and $(dT/dx)_m = 0$. Bearing in mind that $\mu_\omega = \mu_\omega(T)$, we find

$$v = \frac{\lambda}{\rho_0 c_p} \frac{(d^2\Theta/dx^2)_m + (\mu_\omega dS/dx)_m}{(d^2\Theta/dx^2)_m} \quad (14)$$

If the distribution $T(x)$ or $\Theta(x)$ near a point $x = x_m$ is symmetrical, $(d^3\Theta/dx^3)_m = 0$, and we arrive at Eq. (13). However, in a stationary wave the $T(x)$ profile is not symmetrical: Before the maximum, it is steeper than behind the maximum, since the flux accelerates heating of a gas and delays its cooling (see Fig. 12). The quantity $(d^3\Theta/dx^3)_m$, generally speaking, is of the same order as $(\mu_\omega dS/dx)_m$, although its sign is opposite, such that it is difficult to say something ahead of time about the result of deduction of two comparable quantities.

The direct physical cause of a hindered burning of discharge in a parallel beam at very low velocities is associated with the cooling produced by energy losses in a plasma, which is controlled to a certain extent by the attenuation of the light flux. If we digress from the beam attenuation, as was done in Ref. 23, which is quite plausible in the case of weak absorption at $T \sim T_{\text{max}}$ and for small light-channel diameters, $\mu_\omega R \ll 1$, cooling of a plasma, after it was heated to a final temperature T_{max} , may be nearly excluded from consideration and, in this event $v \rightarrow 0$ when S tends to a threshold value $S_{\text{min}} = S_t$. If we digress from the existence of losses—which is plausible in the converse case $\mu_\omega R \gg 1$ —then, regardless of the strong attenuation, the light flux is nevertheless fully absorbed and $v \rightarrow 0$ when $S \rightarrow S_{\text{min}} = 0$ (no losses, no threshold).¹ However, in a general case, as a result of energy losses which become more significant the more rapidly that the heat is released, i.e., S is attenuated, the plasma becomes transparent even before the light flux is fully absorbed. A portion of the light energy remains unused, which inhibits the burning of the discharge. The cooling occurs sooner, the slower the highly-heated plasma drifts into the regions beyond the temperature maximum (the lower the velocity v). The optical thickness of a well-absorbing region is also smaller, which requires that there be more energy initially to provide a proper total energy yield. In this manner, a sharp increase in S_0 occurs when $v \rightarrow 0$. The incomplete utilization of the light energy at low velocities is, thus, responsible for the occurrence of a lower velocity limit. If both attenuation and losses are "included," but it is assumed that the incident flux S_0 is fully absorbed, there is no limit, and $v \rightarrow 0$ when $S_0 \rightarrow S_t > 0$.

All these qualitative rules are especially evident in the case of a simple model of a linearized, one-dimensional regime ($c_p/\lambda = \text{const}$; $\mu_\omega = 0$ when $\Theta < \Theta_0$, μ_ω

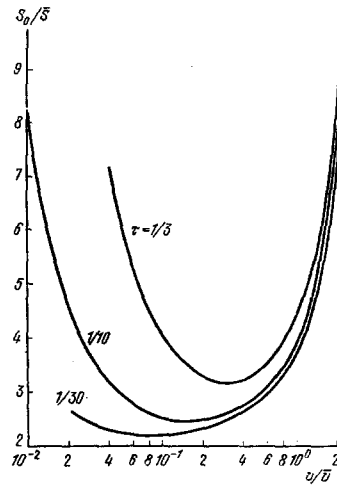


FIG. 16. Radiation intensity required to maintain a stationary one-dimensional regime in an optical-discharge wave as a function of wave propagation velocity, obtained as a result of solving a linearized equation. Curves refer to various values of parameter $\tau = \mu_\omega R/\sqrt{A}$ which characterized relative role of light absorption and energy losses. Curves plotted in dimensionless variables.

$= \text{const}$ when $\Theta > \Theta_0$), which in a general case is described by an equation that follows from Eqs. (10) and (11)

$$\left. \begin{aligned} \frac{\rho_0 c_p v}{\lambda} \frac{d\Theta}{dx} &= \frac{u^2 \Theta}{dx^2} + \delta \mu_\omega S_0 e^{-\mu_\omega x} - \frac{A\Theta}{R^2}, \\ \delta &= \begin{cases} 0 & \text{when } \Theta < \Theta_0, \quad x < 0, \quad x > x_0, \\ 1 & \text{when } \Theta > \Theta_0, \quad 0 < x < x_0, \end{cases} \end{aligned} \right\} \quad (15)$$

and the boundary conditions $\Theta = 0$ when $x = \pm\infty$. At the regional boundaries, when $x = 0$ and $x = x_0$, Θ and $d\Theta/dx$ are continuous.

Equation (15) yields the type of $\Theta(x)$ profile shown in Fig. 12. The desired relationship between flow velocity v and incident beam intensity S_0 , which is responsible for the wave immobility, is expressed by a system of two equations with respect to two unknown parameters v and x_0 . The task narrows down to solving a transcendental equation which yields an intermediate relation between v and x_0 , and calculating the function $S_0(v, x_0)$. In dimensionless variables $\tilde{x} = x/\bar{x}$, where the scales are $\bar{v} = \sqrt{A\lambda}/\rho_0 c_p R$, $\bar{S} = A\Theta_0/\mu_\omega R^2$, and $\bar{x} = R/\sqrt{A}$, the equations for $S_0(v)$ have the following form ($\tau = \mu_\omega R/\sqrt{A}$, a parameter):

$$\left. \begin{aligned} \frac{1 - e^{-(k_1 + \tau)\tilde{x}_0}}{e^{-\tau\tilde{x}_0} - e^{k_2\tilde{x}_0}} &= -\frac{k_1 + \tau}{k_2 + \tau}, \\ k_{1,2} &= \frac{\tilde{v}}{2} \pm \sqrt{1 + \frac{\tilde{v}^2}{4}}, \\ \bar{S} &= \frac{k_1 - k_2}{k_1 + \tau} \frac{1 - \tilde{v}\tau - \tau^2}{e^{-\tau\tilde{x}_0} - e^{k_2\tilde{x}_0}}. \end{aligned} \right\} \quad (16)$$

The results of the calculations are shown in Fig. 16.⁹⁾ The $S_0(v)$ curves are qualitatively similar to the experimental curves in Fig. 15. Asymptotically, when \tilde{v} and $\bar{S} \gg 1$, $\tilde{v} \approx \sqrt{\bar{S}}$, which is in agreement with Eq. (12).

⁹⁾ A numerical solution of the transcendental equation, which proved to be formidable, has been carried out by N. N. Magretova.

When $\bar{v} \rightarrow 0$, but $\tau \neq 0$, the required intensity $\bar{S} \approx 2\tau/3\bar{v} \rightarrow \infty$, which attests to the difficulty of producing a discharge at low velocities. The problem is the smallness of the optical thickness of the absorbing region: $\bar{v} \rightarrow 0$, $\mu_0 \bar{x}_0 \approx 3\bar{v} \rightarrow 0$. In fact, the minimum velocities at which a sharp increase in the intensity occurs in accordance with both calculations and experiment in Ref. 51, are so small, $v \approx 5-7$ cm/s, that determination of threshold values S_t from the analysis of a simplified variant $S(x) = \text{const} = S_0$ —corresponding to an interval $\tau \rightarrow 0$ and extrapolation $S_0(v)$ at $v=0$ —has yielded reasonable results.²³

The solution of Eq. (15) confirms the aforementioned qualitative assertion concerning the fact that the wave velocity in a steady-state regime may not be considered proportional to the heat release gradient at a point of the temperature maximum. For example, when $\tau=0.1$, which in general corresponds to the experimental conditions and $\bar{v}=0.3$, we get $\bar{x}_0=4.81$ and $\bar{S}=2.56$; the dimensionless "temperature" maximum, $\bar{\Theta}_m = \Theta/\Theta_0 = 1.85$, lies at a point $x_m = 2.01$. The dimensionless heat release gradient at the maximum point is -0.209 , and the dimensionless third derivative of Θ , which should have been neglected in order to obtain Eq. (13) from the real Eq. (14), is $+0.149$. The same also applies to other variants.

7. PROJECTS BASED ON THE USE OF OPTICAL DISCHARGES

The possibility of free transmission of laser energy over long distances, the concentration of energy in small volumes by optical means, and high temperature and degree of ionization in the optical discharges all provide perspectives for various applications. Above, we have discussed the possibilities of using continuous optical discharge as a stationary light source of very high brightness, and for the generation of a dense, high-temperature plasma. These have been achieved. In this Section, we shall discuss three projects which are currently considered fictional, although we have watched fiction repeatedly materialize during our lifetimes.

(a) Optical plasmotron as a rocket engine

A system, equivalent to an optical plasmotron shown in Fig. 14, has been proposed as a rocket engine.⁵³ The authors were attracted to the optical discharge because of high temperature. Coupled with the use of the lightest gas, hydrogen, this permits us to obtain inordinately high escape velocities of the plasma v and specific impulses I .¹⁰⁾ Numerical calculations of the light-burning waves in a CO_2 -laser beam were carried out with an allowance for radiative heat transfer and subsequent flow of a plasma in a nozzle. The light channel was considered to be parallel and the radiation intensity was fixed basically at $S_0 = 300$ kW/cm². The radius and selected power are interrelated. If $P_0 = 10$

¹⁰⁾ $I = u/g$, where g is acceleration due to gravity. Heated initially to a temperature T , the gas escapes into the vacuum with a velocity $u \sim \sqrt{kT/M}$, where M is the atomic mass.

kW, $R = 0.1$ cm; if $P_0 = 5$ MW, $R = 2.1$ cm; the radius of the nozzle throat $R_K = 0.4 R$. The maximum temperature at the 30-atm pressure in the inflow attains 19,000 K. The normal propagation velocities (inflow velocities) are $v \sim 2-8$ m/s. The absorption length of laser radiation is 2-3 cm. The plasma velocity in the region of energy release is ~ 1 km/s, and at the throat, ~ 15 km/s. This makes it possible to obtain specific impulses of 1400-2400 s in the case of an escape through the atmosphere, and 4300-4700 s in the case of an escape into the space. Even the best rockets propelled by chemical fuels cannot attain, in the latter case, 500 s; space flight requires specific impulses of 1000-1500 s.

(b) Rocket engine based on the use of recurring explosions from an optical breakdown⁵⁴

In the preceding case it was assumed that a laser is placed aboard the rocket. In this case, laser energy is supplied to a flying vehicle from Earth, a task that is particularly attractive. The engine may function only during take-off of a vehicle through the atmosphere. The tail-end of the vehicle, facing Earth, is designed in the shape of a parabolic mirror. The incident light beam sent from Earth is reflected by the mirror and collected in the focus where it produces an optical air breakdown. The pulsed laser energy is rapidly released in the breakdown plasma, the assumption being that the radiation is beamed in the form of repeating pulses. A "detonation" wave propagates in the air from a point where energy was released; it strikes the mirror surface, is reflected, and in this manner imparts a mechanical impulse to the vehicle (exerts a pressure on it). Detailed calculations have been carried out, the various operational aspects of the engine evaluated, and suitable designs and regimes selected. Of course, to accelerate vehicles of realistic weight, say ~ 100 kg, very high average laser powers are required, which are of the order of 100 MW at the pulse repetition frequency of 300 Hz. It is remarkable that an actual model of such a "laser aero-reactive engine" has been made. A body weighing 5 g was accelerated and moved upward under the effect of a series of optical air breakdowns which were produced by radiation from a small periodically-pulsed CO_2 laser.

(c) Conversion of light into electrical energy⁵⁵

As indicated in selected articles, investigations are in progress concerning different means for converting (aboard a space vehicle) laser energy beamed from Earth into electrical energy to satisfy the energy requirements of artificial satellites. In the preliminary experiments,⁵⁵ this purpose was satisfied by a plasma from a continuous optical discharge. A 6-kW CO_2 laser with a beam diameter of 6 cm was focused by an $f=18$ cm lens in a chamber through which argon under a 1.1-atm pressure was slowly flowing. Thoriated tungsten electrodes were placed on both sides of the optical discharge plasma which was distributed as shown in Fig. 6; one electrode had a small surface and was heated to incandescence to emit electrons, the other, a collector, had a large surface and was cooled by water. A potential difference existed between the electrodes,

evidently due to diffusion of electrons from the plasma to the collector. The voltage-current characteristic of the circuit, including the electrodes and the plasma, was taken. The value of the potential difference ("open circuit" voltage), extrapolated to a zero current, was 1.5 V; the collector was negative. The short circuit current was 0.7 A. If the potential difference (1.5 V) is considered an emf, the electric power is $1.5 \times 0.7 \approx 1$ W, i.e., an efficiency of the order of 0.02%. However, citing a number of investigations, the authors suggest that the conversion efficiency may be significantly improved.

- ¹Yu. P. Raizer, *Lazernaya iskra i rasprostraneniye razryadov* (Laser Spark and Discharge Propagation), Nauka, M., 1974.
- ²P. D. Maker, R. W. Terhune, and C. M. Savage, in III Intern. Conf. on Quant. Electronics, Paris 1963.
- ³D. H. Gill and A. A. Dougal, *Phys. Rev. Lett.* **15**, 845 (1965).
- ⁴A. MacDonald, *Microwave Gas Breakdown* (Russ. transl., Mir, M., 1969).
- ⁵Ya. B. Zel'dovich and Yu. P. Raizer, *Zh. Eksp. Teor. Fiz.* **47**, 1150 (1964) [*Sov. Phys. JETP* **20**, 772 (1965)].
- ⁶M. J. Soileau, *Appl. Phys. Lett.* **35**, 309 (1979).
- ⁷P. Woskoboinikov, W. J. Milligan, H. C. Pradaude, and D. R. Cohn, *Appl. Phys. Lett.* **32**, 527 (1978).
- ⁸N. G. Basov, V. A. Boiko, O. N. Krokhin, and G. V. Sklizkov, *Dokl. Akad. Nauk SSSR* **173**, 538 (1967) [*Sov. Phys. Dokl.* **12**, 248 (1967)].
- ⁹W. F. Hagen, *J. Appl. Phys.* **40**, 511 (1969).
- ¹⁰V. N. Parfenov, L. N. Pakhomov, V. Yu. Petrun'kin, and V. A. Podlevskii, *Pis'ma, Zh. Tekh. Fiz.* **2**, 731 (1976) [*Sov. Tech. Phys. Lett.* **2**, 286 (1976)].
- ¹¹V. D. Zvorykin, F. A. Nikolaev, I. V. Kholin, A. Yu. Chugunov, and A. V. Shelobolin, *Fiz. Plazmy* **5**, 1140 (1979) [*Sov. J. Plasma Phys.* **5**, 638 (1979)].
- ¹²J. P. Caressa, M. Autric, D. Dufresne, and P. Bournot, *J. Appl. Phys.* **50**, 6822 (1979).
- ¹³D. C. Smith and R. G. Meyerand, in: *Principles of Laser Plasmas*, ed. G. Bekefi, N. Y., 1976.
- ¹⁴A. I. Barchukov, F. V. Bunkin, V. I. Konov, and A. A. Lyubin, *Zh. Eksp. Teor. Fiz.* **66**, 965 (1974) [*Sov. Phys. JETP* **39**, 469 (1974)].
- ¹⁵A. M. Bonch-Bruевич, V. I. Zinchenko, and L. N. Kaporskiĭ, *Zh. Tekh. Fiz.* **47**, 1055 (1977) [*Sov. Phys. Tech. Phys.* **22**, 629 (1977)].
- ¹⁶A. Guenther and J. Batis, *TIER* **59**, 277 (1971).
- ¹⁷S. R. Wili and D. A. Tidman, *Appl. Phys. Lett.* **17**, 20 (1970).
- ¹⁸D. W. Koopman and T. D. Wilkerson, *J. Appl. Phys.* **42**, 1883 (1971).
- ¹⁹O. B. Danilov and S. A. Tul'skiĭ, *Zh. Tekh. Fiz.* **48**, 2040 (1978) [*Sov. Phys. Tech. Phys.* **23**, 1164 (1978)].
- ²⁰Yu. P. Raizer, *Osnovy sovremennoi fiziki gazorasryadnykh protsessov* (Fundamentals of the Contemporary Physics of Gas-Discharge Processes), Nauka, M., 1980.
- ²¹Yu. P. Raizer, *Pis'ma Zh. Eksp. Teor. Fiz.* **11**, 195 (1970) [*JETP Lett.* **11**, 120 (1970)].
- ²²N. A. Generalov, V. P. Zimakov, G. I. Kozlov, V. Z. Maslyukov, and Yu. P. Raizer, *ibid.* **11**, 447 (1970) [*ibid.* **11**, 302 (1970)].
- ²³Yu. P. Raizer, *Zh. Eksp. Teor. Fiz.* **58**, 2127 (1970) [*Sov. Phys. JETP* **31**, 1148 (1970)].
- ²⁴Yu. P. Raizer, in XIV Intern. Conf. on Phenomena in Ionized Gases, Grenoble, 1979; *J. de Phys.* **40**, C7-141 (1979).
- ²⁵Yu. P. Raizer, *TVT* **17**, 1096 (1979).
- ²⁶N. A. Generalov, V. P. Zimakov, G. I. Kozlov, V. Z. Maslyukov, and Yu. P. Raizer, *Zh. Eksp. Teor. Fiz.* **61**, 1434 (1971) [*Sov. Phys. JETP* **34**, 763 (1971)].
- ²⁷D. L. Franzen, *Appl. Phys. Lett.* **21**, 62 (1972); *J. Appl. Phys.* **44**, 1927 (1973).
- ²⁸G. I. Kozlov, V. A. Kuznetsov, and V. A. Maslyukov, *Zh. Eksp. Teor. Fiz.* **66**, 954 (1974) [*Sov. Phys. JETP* **39**, 463 (1974)].
- ²⁹D. C. Smith and M. C. Fowler, *Appl. Phys. Lett.* **22**, 500 (1973).
- ³⁰D. R. Keefer, B. B. Henriksen, and W. F. Braerman, *J. Appl. Phys.* **46**, 1080 (1975).
- ³¹M. C. Fowler and D. C. Smith, *J. Appl. Phys.* **46**, 138 (1975).
- ³²G. I. Kozlov, V. A. Kuznetsov, and V. A. Maslyukov, *Fiz. Plazmy* **1**, 830 (1975) [*Sov. J. Plasma Phys.* **1**, 454 (1975)].
- ³³C. D. Moody, *J. Appl. Phys.* **46**, 2475 (1975).
- ³⁴G. I. Kozlov, V. A. Kuznetsov, and V. A. Maslyukov, *Zh. Tekh. Fiz.* **49**, 2304 (1979) [*Sov. Phys. Tech. Phys.* **24**, 1283 (1979)].
- ³⁵Ya. B. Zel'dovich and Yu. P. Raizer, *Fizika udarnykh voln i vysokotemperaturnykh gidrodinamicheskikh yavlenii*. 2-e izd. (Physics of Shock waves and High-Temperature Hydrodynamic Phenomena. 2nd Edit.), Nauka, M., 1966.
- ³⁶N. N. Kozlova, I. E. Markovich, I. V. Nemchinov, A. I. Petrukhin, Yu. E. Pleshanov, V. A. Rybakov, and V. A. Sylyayev, *Kvantovaya Elektron.* **2**, 1930 (1975) [*Sov. J. Quantum Electron.* **5**, 1048 (1975)].
- ³⁷I. Z. Nemtsev, B. F. Mul'chenko, and Yu. P. Raizer, *Pis'ma Zh. Tekh. Fiz.* **2**, 13 (1976) [*Sov. Tech. Phys. Lett.* **2**, 5 (1976)]; I. Z. Nemtsev and B. F. Mul'chenko, *Fiz. plazmy* **3**, 1167 (1977) [*Sov. J. Plasma Phys.* **3**, 649 (1977)].
- ³⁸F. V. Bunkin, V. I. Konov, A. M. Prokhorov, and V. B. Fedorov, *Pis'ma Zh. Eksp. Teor. Fiz.* **9**, 609 (1969) [*JETP Lett.* **9**, 371 (1969)].
- ³⁹J. H. Betteh and D. R. Keefer, *IEEE Trans. Plasma Science* **PS-2**, 122 (1974).
- ⁴⁰G. I. Kozlov and L. K. Selezneva, *Zh. Tekh. Fiz.* **48**, 386 (1978) [*Sov. Phys. Tech. Phys.* **23**, 227 (1978)].
- ⁴¹B. F. Mul'chenko, Yu. P. Raizer, and V. A. Epshtein, *Zh. Eksp. Teor. Fiz.* **59**, 1975 (1970) [*Sov. Phys. JETP* **32**, 1069 (1970)].
- ⁴²L. R. Stegman, J. T. Schriempf, and L. R. Hettche, *J. Appl. Phys.* **44**, 3675 (1973).
- ⁴³E. L. Klosterman and S. R. Byron, *J. Appl. Phys.* **45**, 4751 (1974).
- ⁴⁴J. P. Jackson and P. E. Nielsen, *AIAA Journ.* **12**, 1498 (1974); Russ. transl. in *Raket. tekhn. i kosmonavtika* **12**, 54 (1974).
- ⁴⁵Yu. P. Raizer, *Zh. Eksp. Teor. Fiz.* **48**, 1508 (1965) [*Sov. Phys. JETP* **21**, 1009 (1965)].
- ⁴⁶A. A. Boni and F. Y. Su, *Phys. Fluids* **17**, 340 (1974).
- ⁴⁷F. Y. Su and A. A. Boni, *ibid.* **19**, 960 (1976).
- ⁴⁸V. I. Bergel'son, T. V. Loseva, and I. V. Nemchinov, *PMTEF*, No. 4, 22 (1974); in *Chislennyye metody v fizike plazmy* (Numerical Methods in the Plasma Physics), Nauka, M., 1977.
- ⁴⁹I. V. Nemchinov, A. I. Petrukhin, Yu. E. Pleshanov, and V. A. Rybakov, *Dokl. Akad. Nauk SSSR* **247**, 1368 (1979) [*Sov. Phys. Dokl.* **24**, 655 (1979)].
- ⁵⁰G. I. Kozlov, *Pis'ma Zh. Tekh. Fiz.* **4**, 586 (1978) [*Sov. Tech. Phys. Lett.* **4**, 234 (1978)].
- ⁵¹M. V. Gerastimenko, G. I. Kozlov, V. Z. Kuznetsov, and V. Z. Maslyukov, *ibid.* **5**, 954 (1979) [*ibid.* **5**, 397 (1979)].
- ⁵²H. H. Maecker, *Proc. IEEE* **59**, 439 (1971).
- ⁵³N. H. Kemp and R. G. Root, *J. Spacecraft and Rockets* **16**, 65 (1979); *J. Energy* **3**, 40 (1979); Russ. Transl. *Raket. tekhn. i kosmonavtika* **17**, 128 (1979).
- ⁵⁴F. V. Bunkin and A. M. Prokhorov, *Usp. Fiz. Nauk* **119**, 425 (1976) [*Sov. Phys. Usp.* **19**, 561 (1976)]; V. P. Ageev, A. I. Barchukov, V. F. Bunkin, V. I. Konov, A. M. Prokhorov, A. S. Silenko, and N. I. Chapliev, *Kvantovaya Elektron.* **4**, 2501 (1977) [*Sov. J. Quantum Electron.* **7**, 1430 (1977)].
- ⁵⁵R. W. Thompson, E. J. Manista, and D. L. Alger, *Appl. Phys. Lett.* **32**, 610 (1978); *Laser Focus* **13**, 20 (1977).

Translated by Yuri Ksander
 Edited by R. T. Beyer